Electromagnetically-induced-transparency-related phenomena and their mechanical analogs

J. A. Souza[*]

Departamento de Física, Química e Matemática, Universidade Federal de São Carlos, Sorocaba, São Paulo 18052-780, Brazil
and Departamento de Física, Universidade Federal de São Carlos, São Carlos, São Paulo 13565-905, Brazil

L. Cabral, R. R. Oliveira, and C. J. Villas-Boas

Departamento de Física, Universidade Federal de São Carlos, São Carlos, São Paulo 13565-905, Brazil
(Received 5 December 2014; published 11 August 2015)

Systems of interacting classical harmonic oscillators have received considerable attention in the past years as analog models for describing electromagnetically induced transparency (EIT) and associated phenomena. We review these models and investigate their validity for a variety of physical systems using two and three coupled harmonic oscillators. From the simplest EIT-Λ configuration and two coupled single cavity modes we show that each atomic dipole-allowed transition and a single cavity mode can be represented by a damped harmonic oscillator. Thus, we have established a one-to-one correspondence between the classical and quantum dynamical variables. We show the limiting conditions and the equivalent for the EIT dark state in the mechanical system. This correspondence is extended to other systems that present EIT-related phenomena. Examples of such systems are two- and three-level (cavity EIT) atoms interacting with a single mode of an optical cavity and four-level atoms in a inverted-Y and tripod configurations. The established equivalence between the mechanical and the cavity EIT systems has been corroborated by experimental data. The analysis of the probe response of all these systems also brings to light a physical interpretation for the expectation value of the photon annihilation operator $\langle a \rangle$. We show that it can be directly related to the electric susceptibility of systems, the composition of which includes a driven cavity-field mode.

I. INTRODUCTION

Electromagnetically induced transparency (EIT) is a quantum interference phenomenon responsible for canceling the absorption of a weak probe laser by applying a strong electromagnetic control field in the same medium. In the past decades, much attention has been paid to study EIT and related phenomena, leading to many different applications [1–3]. In its simplest configuration, two electromagnetic fields excite an ensemble of three-level atoms in Λ configuration and the optical properties of the atomic medium are described by the first-order complex electric susceptibility $\chi_e^{(1)}$. Its real part $\mathrm{Re}\{\chi_e^{(1)}\}$ is related to the index of refraction of the medium, featured by a region of anomalous dispersion leading to very small group velocities [4–6]. The zero absorption window is described by the imaginary part $\mathrm{Im}\{\chi_e^{(1)}\}$, which allows applications ranging from high-resolution spectroscopy [2] to atomic clocks [7].

Mechanical and electric analogies of EIT in a Λ configuration and their characteristics in equivalent systems have been noted since Alzar *et al.* [8] reproduced the phenomenology of EIT using two coupled harmonic oscillators and circuit RLC – resistance (R), inductance (L), and capacitance (C). They were inspired by Hemmer and Prentiss [9], who modeled classically the stimulated resonance Raman effect with a set of three coupled classical pendulums. Due to the considerable practical usefulness provided by the classical results, many efforts have been made towards representing EIT-related phenomena in different atomic systems using classical models [10–13]. Its importance has recently grown even more owing to the number of reported classical systems that follow the same dynamics, such as metamaterials [14–19], cavity optomechanics [20–23], multiple coupled photonic crystal cavities [24], acoustic structures [25], coupled resonant systems [26], and so on.

To date, no complete correspondence between the quantum and classical models which yields a direct comparison between the results has been realized. We establish in this work a one-to-one correspondence between the classical and the quantum dynamic variables using two classical coupled harmonic oscillators to model EIT in Λ configuration. We also show the role of a cavity mode in the mechanical system to model EIT-like phenomena observed in two coupled cavity modes and in systems comprised by a single two-level atom interacting with a single mode of a resonator considering two configurations, the driven cavity field and the driven atom. The analysis of the probe response for the driven cavity cases reveals that $\langle a \rangle$ is directly related to the electric susceptibility of the atom-cavity or cavity-cavity systems.

The classical correspondence is also established for EIT-like phenomena observed in four-level atoms in the inverted-Y and tripod configurations and for the cavity EIT (CEIT) system, considering three coupled classical harmonic oscillators. For the atomic tripod configuration we compare the classical analog obtained here with the analog published recently [13], showing the validity of both for different set of parameters. The analog for the CEIT system is presented and the result is compared with an experiment performed with $N \sim 15$ atoms [27]. We show the validity and the limiting conditions to reproduce the quantum results using the classical models. This work can be considerably useful to provide a general mapping of EIT-like systems into a variety of classical systems.

*[*]jamesfisica@gmail.com

II. CLASSICAL ANALOG OF EIT IN DIFFERENT PHYSICAL SYSTEMS USING TWO COUPLED HARMONIC OSCILLATORS

Coupled harmonic oscillators are an intuitive model used as a close analog for many phenomena, including the stimulated resonance Raman effect [9], electromagnetically induced transparency [8,10–13], time-dependent Josephson phenomena [28], adiabatic and nonadiabatic processes [29,30], level repulsion [31], strongly interacting quantum systems [32], one-half spin dynamics [33,34], and coherent quantum states [35–37], among others.

EIT and their classical analogs can be obtained when suitable conditions are prescribed. In what follows, we briefly review some of the EIT-related systems and derive their linear electric susceptibilities from the density matrix formalism. Our focus is to show how the behavior of the electric susceptibility of each atomic system can be reproduced using coupled oscillators through the concept of mechanical susceptibility.

A. The phenomenology of EIT reproduced in two coupled harmonic oscillators

The phenomenon of EIT occurs in three-level atomic systems in Λ configuration with two ground states, $|1\rangle$ and $|2\rangle$, and an excited state, $|3\rangle$, interacting with two classical coherent fields, probe and control, of frequencies ω_p and ω_c, respectively, as illustrated in Fig. 1(a). The atomic transition $|1\rangle \leftrightarrow |3\rangle$ (frequency ω_{31}) is driven by the probe field with Rabi frequency $2\Omega_p$, and the transition $|2\rangle \leftrightarrow |3\rangle$ (frequency ω_{32}) is coupled by the control field with Rabi frequency $2\Omega_c$ [38].
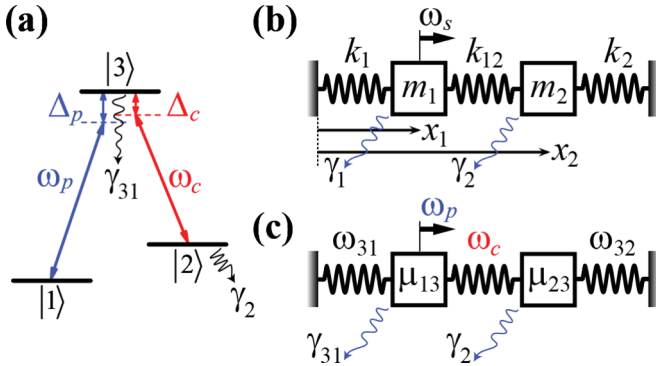

FIG. 1. (Color online) (a) Schematic energy level diagram of a three-level atom in Λ configuration for EIT. It shows two classical electromagnetic fields, probe (ω_p) and control (ω_c), coupling the transitions $|1\rangle \leftrightarrow |3\rangle$ and $|2\rangle \leftrightarrow |3\rangle$, respectively, and their corresponding detunings. The decay rates are represented by $\gamma_{31} = \Gamma_{31} + \Gamma_{32} + \gamma_3$ and γ_2. (b) Coupled damped harmonic oscillators used to reproduce the phenomenology observed in EIT, showing two masses m_1 and m_2 displaced from their equilibrium positions by the distances x_1 and x_2, respectively, attached to three springs with spring constants k_1, k_2, and k_{12}. A driving force of frequency ω_s acts on mass m_1 and the damping constant of the jth harmonic oscillator is represented by γ_j ($j = 1,2$). (c) Classical analog of EIT showing the equivalence of each parameter in the mechanical system. Each harmonic oscillator corresponds to a dipole-allowed transition with electronic dipole moment μ_{i3} ($i = 1,2$).

Introducing the electric dipole and rotating-wave approximations, the time-independent Hamiltonian which describes the atom-field interaction in a rotating frame is given by ($\hbar = 1$) [3]

$$H = (\Delta_p - \Delta_c)\sigma_{22} + \Delta_p \sigma_{33} - (\Omega_p \sigma_{31} + \Omega_c \sigma_{32} + \text{H.c.}),$$
(1)

where $\sigma_{ij} = |i\rangle\langle j|, i,j = 1,2,3$ are the atomic raising and lowering operators ($i \neq j$), and atomic energy-level population operators ($i = j$). The detunings are given by $\Delta_p = \omega_{31} - \omega_p$, $\Delta_c = \omega_{32} - \omega_c$ and H.c. stands for the Hermitian conjugate. The dynamics of the system is obtained by solving the master equation for the atomic density operator (ρ),

$$\dot{\rho} = -i[H,\rho] + \sum_{m=1,2} \Gamma_{3m}(2\sigma_{m3}\rho\sigma_{3m} - \sigma_{33}\rho - \rho\sigma_{33})$$

$$+ \sum_{n=2,3} \gamma_n(2\sigma_{nn}\rho\sigma_{nn} - \sigma_{nn}\rho - \rho\sigma_{nn}),$$
(2)

where Γ_{31}, Γ_{32} are the polarization decay rates of the excited level $|3\rangle$ to the levels $|1\rangle$ and $|2\rangle$ and γ_2, γ_3 the nonradiative atomic dephasing rates of states $|2\rangle$ and $|3\rangle$, respectively.

It is assumed that all N atoms contained in a volume V couple identically to the electromagnetic fields and that the medium is isotropic and homogenous. Considering that the atoms do not interact with each other and ignoring local-field effects, the optical response of the medium to the applied probe field $E(t) = E_p e^{-i\omega_p t} + \text{c.c.}$ can be obtained through the expectation value of the atomic polarizability,

$$\mathbf{P}(t) = \chi_e^{(1)}\mathbf{E}(t),$$
(3)

with $\chi_e^{(1)}$ denoting the linear electric susceptibility. The polarization can also be written in terms of the expectation value of the dipole moment operator μ per unit volume

$$\mathbf{P}(t) = -\frac{1}{V}\sum_{i=1}^{N}\langle e\mathbf{r}_i(t)\rangle = \frac{N}{V}\text{Tr}(\mu\rho).$$
(4)

In this way the linear response of the probe beam in the atomic sample can be directly related to the off-diagonal density matrix element ρ_{31},

$$\chi_e^{(1)}(\omega_p) = \frac{N|\mu_{13}|}{V E_p}\rho_{31}.$$
(5)

From Eqs. (1) and (2) the full equations of motion for the density matrix are given by

$$\dot{\rho}_{31} = -i\{(\Delta_p - i\gamma_{31})\rho_{31} - \Omega_p(\rho_{11} - \rho_{33})\} + i\Omega_c\rho_{21}, \quad (6a)$$

$$\dot{\rho}_{21} = -i\{[(\Delta_p - \Delta_c) - i\gamma_2]\rho_{21} + \Omega_p\rho_{23}\} + i\Omega_c\rho_{31}, \quad (6b)$$

$$\dot{\rho}_{23} = -i\{[-\Delta_c - i(\gamma_{31} - \gamma_2)]\rho_{23} + \Omega_p\rho_{21}\} + i\Omega_c(\rho_{33} - \rho_{22}), \quad (6c)$$

where $\gamma_{31} = \Gamma_{31} + \Gamma_{32} + \gamma_3$.

As described in detail by Fleischhauer *et al.* [3], EIT occurs when the population of the system is initially in the ground state $|1\rangle$. The state of zero absorption, referred to as the dark state, is usually attributed to the result of quantum interference between two indistinguishable paths. This state corresponds to $|1\rangle$ if the conditions $\Omega_p \ll \Omega_c$ and $\gamma_2 \ll \gamma_{31}$ are prescribed to

yield $\rho_{11} \approx 1$ and consequently $\rho_{22} \approx 0$. The state $|3\rangle$ is never populated ($\rho_{33} = 0$) in the dark state. Using these conditions in Eqs. (6), the steady-state solutions ($\dot\rho_{ij} = 0$) for ρ_{21} and ρ_{31} can be determined through the equations

$$(\Delta_p - i\gamma_{31})\rho_{31} - \Omega_c\rho_{21} = \Omega_p, \tag{7a}$$

$$(\delta - i\gamma_2)\rho_{21} - \Omega_c\rho_{31} = 0, \tag{7b}$$

yielding

$$\rho_{31}(\omega_p) = \frac{\Omega_p(\delta - i\gamma_2)}{(\Delta_p - i\gamma_{31})(\delta - i\gamma_2) - \Omega_c^2}, \tag{8}$$

where we have introduced the two-photon detuning $\delta = \Delta_p - \Delta_c$.

Hereafter, the susceptibility stated in Eq. (5) is replaced with a reduced susceptibility that does not depend on the specific details of the physical system. Then, for EIT it reads

$$\tilde\chi_e(\omega_p) = \frac{VE_p}{N|\mu_{13}|}\chi_e^{(1)}(\omega_p) = \rho_{31}(\omega_p). \tag{9}$$

Thus, the main characteristics of EIT regarding absorption, gain, and the control of the group velocity of light in a medium can be obtained from the imaginary and real parts of ρ_{31}.

Note that the essential features of EIT are derived using a semiclassical model, where it is assumed that two classical fields are interacting with an atomic ensemble with microscopic coherences treated quantum mechanically. Under the assumption of low atomic excitation ($\rho_{11} \approx 1$), which is experimentally justified by choosing an appropriately low pump intensity, implying that $\Omega_p \ll \Omega_c$, effects of atomic saturation are neglected. In this way, the expectation values of the atomic operators $\rho_{ij} = \langle\sigma_{ji}\rangle$ can be replaced with classical amplitudes.

The mechanical model used to demonstrate the classical analog of EIT consists of two coupled, damped harmonic oscillators with one of them driven by a harmonic force $F_s(t) = Fe^{-i(\omega_s t + \phi_s)} + $ c.c., for $\phi_s = 0$ and frequency ω_s [8]. Considered are two particles 1 and 2 with equal masses $m_1 = m_2 = m$ and three springs arranged as illustrated in Fig. 1(b). The two outside spring constants are k_1 and k_2. The third spring couples linearly the two particles and its constant spring is k_{12}. It is assumed that the whole system moves in only one dimension x and the distances x_1 and x_2 measure the displacements of particles 1 and 2 from their respective equilibrium positions. The equations of motion for the two masses are

$$m\ddot x_1 = -k_1 x_1 - \eta_1\dot x_1 - k_{12}(x_1 - x_2) + F_s(t), \tag{10a}$$

$$m\ddot x_2 = -k_2 x_2 - \eta_2\dot x_2 - k_{12}(x_2 - x_1), \tag{10b}$$

which are usually written as

$$\ddot x_1 + \omega_1^2 x_1 + 2\gamma_1\dot x_1 - \omega_{12}^2 x_2 = \frac{F_s(t)}{m}, \tag{11a}$$

$$\ddot x_2 + \omega_2^2 x_2 + 2\gamma_2\dot x_2 - \omega_{12}^2 x_1 = 0, \tag{11b}$$

where $\omega_j^2 = (k_j + k_{12})/m$, $\omega_{12}^2 = k_{12}/m$, and the damping constant of the jth harmonic oscillator is $2\gamma_j = \eta_j/m$, $j = 1,2$. Assuming that the steady-state solution of equations above

has the form $x_j = N_j e^{-i\omega_s t} + $ c.c., we find

$$\left(-\omega_s^2 + \omega_1^2 - 2i\gamma_1\omega_s\right)N_1 - \omega_{12}^2 N_2 = \frac{F}{m}, \tag{12a}$$

$$\left(-\omega_s^2 + \omega_2^2 - 2i\gamma_2\omega_s\right)N_2 - \omega_{12}^2 N_1 = 0, \tag{12b}$$

where the complex conjugate solution (c.c.) was omitted for simplicity. Note that Eqs. (12) for N_1 and N_2 have the same structure as Eqs. (7) for ρ_{31} and ρ_{21}, respectively.

Solving Eqs. (12) for the displacement of the driven oscillator $x_1(t)$ and considering ω_s near to the natural oscillation frequencies ω_j ($j = 1,2$), so that $\omega_j^2 - \omega_s^2 \approx 2\omega_j(\omega_j - \omega_s)$ and $\gamma_j\omega_s \approx \gamma_j\omega_j$, we have

$$x_1(t) \simeq \frac{F/(2m\omega_1)(\Delta_2 - i\gamma_2)}{(\Delta_1 - i\gamma_1)(\Delta_2 - i\gamma_2) - \Omega_{12}^2}e^{-i\omega_s t} + \text{c.c.}, \tag{13}$$

where we have defined the detunings $\Delta_j = \omega_j - \omega_s$ and the classical coupling rate between particles 1 and 2 as $2\Omega_{12} = \omega_{12}^2/\sqrt{\omega_1\omega_2}$, in analogy to the Rabi frequency of the control field ($2\Omega_c$). The quantity $F/m\omega_1 = 2\Omega_s C_1$ has dimension of frequency ($2\Omega_s$) times length (C_1). The first term makes the role of the Rabi frequency of the probe field ($2\Omega_p$). Then, Eq. (13) can be reduced to the form

$$x_1(t) = C_1\rho_{co}e^{-i\omega_s t} + \text{c.c.}, \tag{14}$$

where the dimensionless complex amplitude ρ_{co} is given by

$$\rho_{co}(\omega_s) = \frac{\Omega_s(\Delta_2 - i\gamma_2)}{(\Delta_1 - i\gamma_1)(\Delta_2 - i\gamma_2) - \Omega_{12}^2}. \tag{15}$$

An equation similar to (14) can be derived for the atomic system by making $|\mathbf{r}_i(t)| = x(t)$ in Eq. (4) for $N = 1$ and using Eq. (3), Eq. (5), and the expression for the applied probe field $E(t) = E_p e^{-i\omega_p t} + $ c.c., yielding

$$x(t) = C_2\rho_{31}e^{-i\omega_p t} + \text{c.c.} = C_2\tilde\chi_e e^{-i\omega_p t} + \text{c.c.}, \tag{16}$$

where $C_2 = |\mu_{13}|/e$, similarly to C_1, bears dimension of length. By comparing Eq. (14) with the first equality of Eq. (16) we find the analog $C_1 \equiv C_2$, $\omega_s \equiv \omega_p$, and $\rho_{co} \equiv \rho_{31}$. The analog is obtained for the steady-state solution of both systems, EIT and coupled oscillators. In Sec. 1 of the Appendix we used the Hamiltonian formalism to show that the dynamics of the EIT system, given by $\dot\rho_{31}$ and $\dot\rho_{21}$, is also similar to the dynamics of the classical oscillators. This formalism is also advantageous to obtain a direct definition of the classical pumping rate Ω_s as a function of the parameters of the mechanical system, which is $\Omega_s = \sqrt{F^2/2m\omega_1}$, meaning that $C_1 = \sqrt{1/2m\omega_1}$.

In analogy to the EIT system, Eq. (16), we define a reduced mechanical susceptibility $\tilde\chi_M(\omega_s) = \rho_{co}(\omega_s)$. The concept of susceptibility of a mechanical oscillator is widely used in optomechanics [20–23]. Here we are extending this idea to a set of coupled oscillators. By inspection in Eqs. (8) and (15) we see that ρ_{31} and ρ_{co} are perfectly equivalent. Thus, the classical analog of each parameter of EIT in atomic physics can be identified formally in the mechanical system, as summarized in Table I and illustrated in Fig. 1(c). Each harmonic oscillator is identified as a dipole-allowed transition with electronic dipole moment μ_{i3} ($i = 1,2$).

TABLE I. Classical analog of EIT using two mechanical coupled harmonic oscillators (2-MCHO).

EIT (ρ_{31})	2-MCHO (ρ_{co})
Δ_p	Δ_1
δ	Δ_2
Ω_p	Ω_s
Ω_c	Ω_{12}
γ_{31}	γ_1
γ_2	γ_2

The classical analog for the two-photon detuning $\delta = \Delta_p - \Delta_c$ is $\Delta_2 = \Delta_1 - \Delta_{21}$, where Δ_{21} accounts for the detuning of the resonant frequencies between oscillator 2 and oscillator 1. It can be obtained readily by setting $k_2 = k_1 \pm \Delta k$. The detuning Δ_{21} is responsible for reproducing the shift observed in the dark state when $\Delta_c \neq 0$. The atomic transitions of the EIT system are considered to have fixed resonant frequencies ω_{31} and ω_{32}, meaning that the detuning Δ_c is performed by changing the frequency of the control field ω_c. In the mechanical system the equivalent of ω_c is ω_{12} but the classical detuning Δ_{21} is performed by changing the spring constants k_1 or k_2 and not k_{12}. This is because ω_1 and ω_2 depends on k_{12} in the same way. Then we have to keep ω_{12} constant by fixing k_{12} and change the resonant frequencies ω_1 and ω_2 through k_1 and k_2 to produce the detuning Δ_{21}. For perfect control field resonance $\Delta_c = 0$, we have $\delta = \Delta_p$, which corresponds to $\Delta_1 = \Delta_2$ in Eq. (15), implying that $\omega_1 = \omega_2$ and, consequently, $k_1 = k_2$ for the coupled oscillators.

In Fig. 2 we show the imaginary and real parts of the reduced electric susceptibility $\tilde{\chi}_e$ vs the normalized probe-
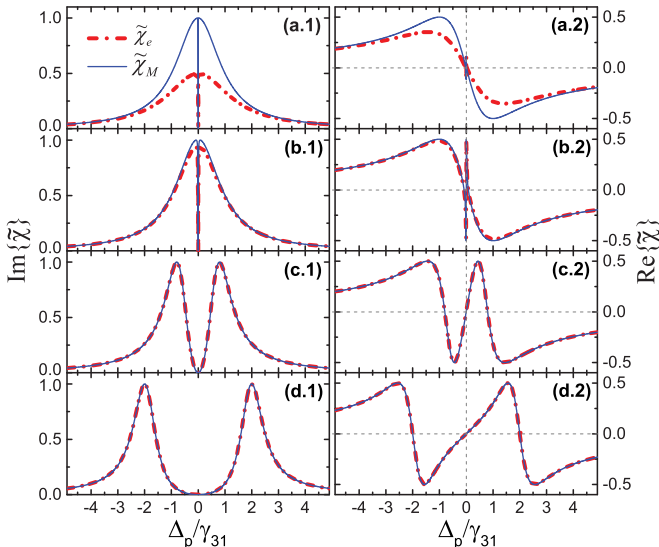

FIG. 2. (Color online) Imaginary and real parts of the reduced electric susceptibility $\tilde{\chi}_e$ vs the normalized probe-atom detuning Δ_p/γ_{31} for the EIT system in comparison with its classical counterpart $\tilde{\chi}_M$ for $\Omega_p = 0.02\gamma_{31}$, $\gamma_2 = 0$, $\Delta_c = 0$, and different values of the Rabi frequency of the control field (a) $\Omega_c = 0.02\gamma_{31}$, (b) $0.08\gamma_{31}$, (c) $0.8\gamma_{31}$, and (d) $2.0\gamma_{31}$. For the mechanical system we use the same set of parameters following the analog presented in Table I.

atom detuning Δ_p/γ_{31} for the EIT system in comparison with its mechanical counterpart $\tilde{\chi}_M$, obtained using two coupled oscillators. The parameters in the classical system are set to be the same as in the EIT following the analog presented in Table I, for $\Omega_p = 0.02\gamma_{31}$, $\gamma_2 = 0$, $\Delta_c = 0$, and different values of the Rabi frequency of the control field Ω_c.

For the set of parameters used in Figs. 2(a) and 2(b) the EIT condition $\Omega_p \ll \Omega_c$ is not deeply satisfied. Once $\rho_{11} \neq 1$ in these cases, the classical model does not reproduce the atomic result satisfactorily. When the condition is fulfilled, $\rho_{11} \approx 1$, we have perfect equivalence between the classical and semiclassical results, as depicted in Figs. 2(c) and 2(d).

If the EIT condition $\Omega_p \ll \Omega_c$ is deeply satisfied, the absorption profile of EIT presented in Fig. 2, for $\gamma_2 = 0$, remains observable even for nonvanishing γ_2, since the condition $\gamma_2 \ll \gamma_{31}$ is prescribed [3]. In this way, the classical model reproduces the atomic system for any set of parameters.

If we recall the dressed-states analysis for EIT, the dark state, given by the transparency window observed between the two peaks of absorption, is written as the superposition between the bare ground states $|1\rangle$ and $|2\rangle$ and not the excited state $|3\rangle$. This means that an atom in this state has no probability of absorbing or emitting a photon. The idea of quantum interference process behind the cancellation of absorption in EIT systems is widely described in the literature [1–3]. When classical analogies for such systems are presented, like the one we are discussing here, many questions arise: What physical property is transparent for the coupled oscillators? What is interfering in this system? And, most importantly, what is the classical dark state in this case?

The first question was already addressed by Alzar *et al.* [8]. They showed that the classical observable related to the EIT absorption profile is given by the real part of the average power absorbed by oscillator 1, owing the application of the harmonic force $F_s(t)$, while the dispersive behavior is contained in the real part of the frequency dependence of the amplitude of x_1. Note that these observables are in full agreement with our definition of the reduced mechanical susceptibility $\tilde{\chi}_M(\omega_s) = \rho_{co}(\omega_s)$. The power absorbed by oscillator 1 is given by $P_s(t) = F_s(t)\dot{x}_1(t) = -i\omega_s F_s(t)x_1(t)$. The relation between P_s and ρ_{co} is drawn from Eq. (14) through $x_1(t)$. Once P_s is multiplied by the imaginary number i, the imaginary part of ρ_{co} depicted in Fig. 2 is related to the real part of P_s. Equation (14) also provides a straightforward relation between the dispersive behavior, defined by Alzar, and the real part of ρ_{co} in Fig. 2 once ρ_{co} is contained in the amplitude of x_1.

In analogy to the dressed-states analysis, if we recall the normal modes description for the coupled oscillators system, we can answer the remaining questions readily. All calculations are described in detail in Sec. 2 of the Appendix. Considering the simplified case where $m_{1,2} = m$, $k_{1,2} = k$, and the definition of the normal coordinates X_+ and X_-, which are linear combinations of $x_1(t)$ and $x_2(t)$, the coupled Hamiltonian (A1), described in Sec. 1 of the Appendix, can be written as a combination of two uncoupled forced harmonic oscillators with normal resonance frequencies $\omega_+ = \sqrt{k/m}$ and $\omega_- = \sqrt{\omega_+^2 + 2\omega_{12}^2}$. These are the resonance frequencies of the two normal modes of the system, usually named as the symmetric $NM_{(+)}$ and asymmetric $NM_{(-)}$ modes. In $NM_{(+)}$

both masses move in exactly the same way, meaning that the middle spring is never stretched, while in $NM_{(-)}$ the masses move oppositely. This means that any arbitrary motion of the system, like the displacement of oscillator 1 or 2, is a linear combination of those two normal modes. In other words, $x_{1,2}(t)$ can be seen as a superposition of two harmonic motions.

The EIT-like profile is observed when the damping forces are considered. In this case Eqs. (A11) in Sec. 2 of the Appendix for the normal modes become coupled through the damping constants γ_1 and γ_2. Solving for the steady-state solution we find a relationship between the normal coordinates X_+ and X_-, which depends on the frequencies of the normal modes $\omega_\pm$, the frequency of the force ω_s, and the damping constant of oscillator 2, γ_2; see Eq. (A12). As we are probing the response of oscillator 1 due to the harmonic force $F_s(t)$, the classical dark state is observed when $\omega_s = \omega_1$, with $\omega_1^2 = \omega_+^2 + \omega_{12}^2$. Note that the frequency ω_1 sits in the range between ω_+ and ω_-, which is a region of high probability of interference between the normal modes.

As we have discussed, the EIT transparency window, which characterizes the dark state, is observed when the conditions $\Omega_p \ll \Omega_c$ and $\gamma_2 \ll \gamma_{31}$ are prescribed. According to Table I the classical analog for these conditions are $\Omega_s \ll \Omega_{12}$ and $\gamma_2 \ll \gamma_1$. Considering $\gamma_2 \to 0$, as in Fig. 2, and $\omega_s = \omega_1$, we find that $X_+ = -X_-$. Once the displacement of oscillators 1 and 2 are given by $x_{1,2} = \sqrt{2}/2(X_+ \pm X_-)$, we have $x_1 = 0$ and $x_2 \neq 0$ in this case. From Eq. (14) $x_1 = 0$ is fulfilled for $\rho_{co} = 0$, as observed in Fig. 2 for zero detuning. Thus, the classical dark state is obtained when oscillator 1 stays stationary while oscillator 2 oscillates harmonically. In other words, oscillator 1 becomes transparent to the effect of the driving force for $\omega_s = \omega_1$ conducting to zero power absorption, which is a consequence of a destructive interference between the two normal modes $NM_{(\pm)}$ in the displacement of oscillator 1.

The first classical condition $\Omega_s \ll \Omega_{12}$ becomes necessary for small but nonzero γ_2, i.e., $\gamma_2 \ll \gamma_1$. In this case the classical dark state remains observable for $k_{12} \gg k_1$, meaning that $X_+ \approx -X_-$; see Eq. (A13) in Sec. 2 of the Appendix. From the definitions of Ω_s and Ω_{12} one can find readily that $\Omega_s = F\sqrt{\Omega_{12}/k_{12}}$, showing that the relation between Ω_s and Ω_{12} also depends on F, as expected. Similarly to the atomic system, where the probe field is turned on slowly for the state $|1\rangle$ evolving into the dark state and decouples from the other states, in the classical system the strength of the force, given by the amplitude F, is also too small to guarantee the usual approximation of small oscillations. Then if F is relatively small and $k_{12} \gg k_1$, we have the condition $\Omega_s \ll \Omega_{12}$ for nonvanishing γ_2 but $\gamma_2 \ll \gamma_1$. Thus, the conditions to observe the phenomenology of EIT can be completely mapped onto the classical system composed of two coupled damped harmonic oscillators, showing that $\text{Im}\{\tilde{\chi}_e(\omega_p)\} \equiv \text{Im}\{\tilde{\chi}_M(\omega_s)\}$ and $\text{Re}\{\tilde{\chi}_e(\omega_p)\} \equiv \text{Re}\{\tilde{\chi}_M(\omega_s)\}$, since $\Omega_p \ll \Omega_c$ and $\gamma_2 \ll \gamma_{31}$.

The similarities obtained between the EIT atomic system and the mechanical coupled oscillators are not surprising. Many aspects of the atom-field interaction can be described by the classical theory of optical dispersion [39,40]. According to this theory, systems which can be approximated by two discrete levels are represented as classical harmonic oscillators. Then the classical picture of a two-level atomic system consists of a

massive positive nucleus surrounded by an electron cloud with an equal negative charge. The electron of charge q and mass m is supposed to be bound to the immovable nucleus by a linear restoring force $-kx$, where x is the distance between their centers of mass and charge. For the static case these centers are coincident and the atom has zero dipole moment. The energy loss is introduced phenomenologically as a damping force proportional to velocity $-\eta\dot{x}$. If the atom is disturbed by an electromagnetic field E, there is also an applied force on the electron $F_q = qE$, and then the electron cloud oscillates along the center of mass. Thus, we have an oscillating dipole with dynamics described by the same equation of motion of a forced, damped harmonic oscillator, $m\ddot{x} + \eta\dot{x} + kx = F_q$, which is the same obtained previously for the first oscillator if $k_{12} = 0$. Once the EIT phenomenon is observed in an ensemble of noninteracting three-level atoms in their ground states, it provides an instructive example of the extension of the classical theory of optical dispersion for multilevel systems. Each atomic transition behaves as a harmonic oscillator which loses energy by some mechanical friction mechanism.

If we turn back to the physical analogy between EIT and the classical model reported by Alzar *et al.* [8], the atom is represented by oscillator 1. According to the classical theory presented previously, this would be correct if the atom has two discrete levels of energy, i.e., only one dipole-allowed transition, which is not the case. As we are dealing with three-level atoms, it is correct to represent each dipole transition as a harmonic oscillator. According to the classical picture for the atom, displayed in Fig. 1(c), the dipole transition frequencies ω_{31} and ω_{32} correspond to the natural frequencies of particles 1 and 2, respectively. The analog for the control and probe fields are equivalent to those presented in Ref. [8], where they are identified by the coupling spring and by the harmonic force acting on particle 1, respectively.

For other classical systems, like RLC coupled circuits and acoustic structures, the analog of the EIT absorption is also obtained from the real part of the power absorbed by the pumped oscillator [8,10–13].

In what follows the classical analog for different quantum systems are presented using the same configuration for the two mechanical coupled harmonic oscillators model discussed here.

B. EIT-like phenomenon in two coupled optical cavities

Once we can reproduce the phenomenology of EIT with two classical coupled oscillators it is natural to consider the oscillators quantum mechanically and see the consequences of it in the EIT-like phenomenon and its conditions [41]. For this end, we used a model consisting of two coupled optical cavities with one of them pumped by a coherent field. The use of optical cavities is convenient because we show the classical analog for EIT-related phenomena in systems composed of a single two- or three-level atom coupling a single mode of an optical resonator.

The two single electromagnetic modes of frequencies $\omega_{\text{cav}}^{(a)}$ and $\omega_{\text{cav}}^{(b)}$ of optical resonators a and b, respectively, exchange energy with Rabi frequency 2λ. Cavity a is driven by a coherent field (probe) of frequency ω_p and strength ε, as illustrated in Fig. 3(a).
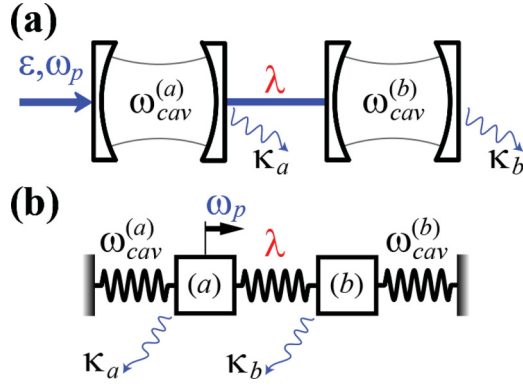
FIG. 3. (Color online) (a) Two coupled cavities showing their respective single cavity modes with frequencies $\omega_{\text{cav}}^{(a)}$, $\omega_{\text{cav}}^{(b)}$ and cavity decay rates κ_a, κ_b. Cavity a is driven by a classical probe field with frequency ω_p and strength ε. The electromagnetic modes exchange energy with Rabi frequency 2λ. (b) Classical analog showing the equivalence for each parameter of the coupled cavity modes in the mechanical system.

Introducing the rotating-wave approximation (RWA) and considering identical frequencies $\omega_{\text{cav}}^{(a)} = \omega_{\text{cav}}^{(b)} = \omega_{\text{cav}}$ for simplicity, the time-independent Hamiltonian which describes the cavity-cavity coupling in the probe laser rotating frame is given by

$$H = \Delta_{\text{cav}}(a^\dagger a + b^\dagger b) + \lambda(ab^\dagger + a^\dagger b) + \varepsilon(a + a^\dagger). \quad (17)$$

Since the cavity modes are quantized, they are expressed in terms of creation ($a^\dagger, b^\dagger$) and annihilation (a, b) operators. $\Delta_{\text{cav}} = \omega_{\text{cav}} - \omega_p$ is the probe-cavity detuning. The master equation for the cavity-cavity density operator is

$$\dot{\rho} = -i[H, \rho] + \sum_{\alpha=a,b} \kappa_\alpha(2\alpha\rho\alpha^\dagger - \alpha^\dagger\alpha\rho - \rho\alpha^\dagger\alpha), \quad (18)$$

where κ_α is the cavity mode decay rate of cavity α. The time evolution for the expectation value of the field operators are

$$\langle\dot{a}\rangle = -i\{(\Delta_{\text{cav}} - i\kappa_a)\langle a\rangle + \lambda\langle b\rangle + \varepsilon\}, \quad (19a)$$

$$\langle\dot{b}\rangle = -i\{(\Delta_{\text{cav}} - i\kappa_b)\langle b\rangle + \lambda\langle a\rangle\}, \quad (19b)$$

which exhibits essentially the same structure as Eqs. (A5), Sec. 1 of the Appendix, for $\dot{\rho}_\alpha$ and $\dot{\rho}_\beta$, respectively, in the description of the dynamics of the coupled oscillators system.

Once the cavity mode a absorbs photons from the pumping field and communicates them to cavity b, through the coupling λ, we represent the probe response of the cavity-cavity system as a reduced electric susceptibility given by the expectation value of the driven cavity field, i.e., $\tilde{\chi}_{CC}(\omega_p) = \langle a\rangle$. Note that it is precisely what was done for the EIT medium, where $\tilde{\chi}_e(\omega_p) = \rho_{31}$. A formal correspondence between ρ_{31} in atomic physics and the intracavity field $\langle a\rangle$ was already pointed out by Weiss *et al.* in their work about optomechanically induced transparency [22].

The steady-state solutions of the expectation value of field operators in Eqs. (19) provide the solution for the intracavity field of cavity a,

$$\langle a\rangle = \frac{-\varepsilon(\Delta_{\text{cav}} - i\kappa_b)}{(\Delta_{\text{cav}} - i\kappa_a)(\Delta_{\text{cav}} - i\kappa_b) - \lambda^2}, \quad (20)$$

TABLE II. Classical analog of EIT-like in two coupled cavity modes (EIT-CCM) using two mechanical coupled harmonic oscillators (2-MCHO).

EIT-CCM ($\langle a\rangle$)	2-MCHO (ρ_{co})
Δ_{cav}	Δ_s
ε	Ω_s
λ	Ω_{12}
κ_a	γ_1
κ_b	γ_2

which is identical to the reduced mechanical susceptibility $\tilde{\chi}_M(\omega_s) = \rho_{co}$ obtained for the two coupled harmonic oscillators in Eq. (15) for $\Delta_1 = \Delta_2 = \Delta_s$. The negative signal observed in Eq. (20) can be reproduced from the classical equations by considering the phase $\phi_s = \pi$ in the applied force on oscillator 1, which is equivalent to making $-F$ in Eq. (15). Once it is considered only one force in the classical analog, the phase is not relevant. Nonetheless, it becomes important for atomic systems with more than three levels, like in the four-level tripod configuration we show afterwards, in which the classical analog is obtained by considering two oscillating forces out of phase by π.

The classical analog of each parameter of the coupled cavity modes is summarized in Table II. The CEIT-like condition is given by $\varepsilon \ll \lambda$ and $\kappa_b \ll \kappa_a$ and the classical analog is obtained for any set of parameters.

The agreement between the cavity-field and oscillator-force responses is somehow expected. In the quantum theory of radiation [42] a general multimode field is represented by a collection of harmonic oscillators, one for each mode. Then, the single mode of the electromagnetic field of cavity a or b is dynamically equivalent to a simple harmonic oscillator. Once we have two coupled cavity modes, naturally it will be equivalent to two coupled oscillators.

Narducci *et al.* [43] showed that differences in the dynamics of two coupled quantum oscillators may arise between the approximated Hamiltonian given by Eq. (17) and its exact solution, where the counter-rotating-wave terms $a^\dagger b^\dagger$ and ab are considered. They established the limits of validity of the RWA in terms of the strength of coupling λ. Our results show that if the RWA is assumed to be valid, the quantum dynamics of two coupled cavity modes can be reproduced by the classical dynamics of two coupled harmonic oscillators. Thus, to obtain the classical analog for systems which involve a cavity mode, we can represent it as a harmonic oscillator with natural frequency ω_{cav}, similarly to an atomic dipole-allowed transition in the low atomic excitation condition.

The result obtained in Eq. (20) goes beyond the perfect agreement between quantum and classical models. It opens the possibility of a physical interpretation for the expectation value of the photon annihilation operator $\langle a\rangle$, showing that it is directly related to the electric susceptibility of a cavity mode. In what follows we show that this interpretation can also be used for systems composed of two- and three-level atoms interacting with a single cavity mode driven by a coherent field.

C. EIT-like phenomena in two-level atom coupled to an optical cavity mode

The absorption spectrum of EIT is also observed when a single two-level atom is coupled to a single cavity mode. This effect was predicted by Rice and Brecha [44] and termed as cavity-induced transparency (CIT). They found that under specific conditions an atom-cavity transmission window, usually referred to as intracavity dark state, arises as a consequence of quantum interference between two absorption paths and not as a result of vacuum-Rabi splitting. They showed an analogous configuration in the weak-probe limit considering the driven cavity and the driven atom cases. We examine both configurations and show their classical equivalent using two coupled oscillators.

First we consider the driven cavity case. The system is composed of a single atom with two energy levels, $|g\rangle$ and $|e\rangle$, coupled to a single electromagnetic mode of frequency ω_{cav} of an optical resonator. The cavity is driven by a coherent field (probe) with frequency ω_p and strength ε_c. The atomic transition $|g\rangle \leftrightarrow |e\rangle$ (frequency ω_0) is coupled by the cavity mode with vacuum Rabi frequency $2g$. The time-independent Hamiltonian which describes the atom-field coupling in a rotating frame is obtained using the driven Jaynes-Cummings model,

$$H = \Delta_0 \sigma_{ee} + \Delta_c a^\dagger a + g(a\sigma_{eg} + a^\dagger \sigma_{ge}) + \varepsilon_c(a + a^\dagger), \quad (21)$$

with detunings given by $\Delta_0 = \omega_0 - \omega_p$, $\Delta_c = \omega_{\text{cav}} - \omega_p$.

The master equation for the atom-cavity density operator is

$$
\begin{aligned}
\dot{\rho} = &-i[H,\rho] + \kappa(2a\rho a^\dagger - a^\dagger a\rho - \rho a^\dagger a) \\
&+ \Gamma_{eg}(2\sigma_{ge}\rho\sigma_{eg} - \sigma_{ee}\rho - \rho\sigma_{ee}) \\
&+ \gamma_e(2\sigma_{ee}\rho\sigma_{ee} - \sigma_{ee}\rho - \rho\sigma_{ee}),
\end{aligned} \quad (22)
$$

where κ is the cavity-field decay rate, Γ_{eg} the polarization decay rate of the excited level $|e\rangle$ to the level $|g\rangle$, and γ_e the nonradiative atomic dephasing rate of state $|e\rangle$. By using the commutation relation $[a,a^\dagger] = 1$ and considering perfect atom-cavity resonance $\omega_0 = \omega_{\text{cav}}$, implying that $\Delta_0 = \Delta_c$, the time evolution of the expected values of the atomic and field operators are given by

$$\langle \dot{a} \rangle = -i\{(\Delta_c - i\kappa)\langle a \rangle + g\langle \sigma_{ge} \rangle + \varepsilon_c\}, \quad (23a)$$

$$\langle \dot{\sigma}_{ge} \rangle = -i\{(\Delta_c - i\gamma_{eg})\langle \sigma_{ge} \rangle - g\langle a \rangle \langle \sigma_z \rangle\}, \quad (23b)$$

where $\gamma_{eg} = \Gamma_{eg} + \gamma_e$ and $\langle \sigma_z \rangle = \langle \sigma_{ee} \rangle - \langle \sigma_{gg} \rangle$.

The closed set of coupled equations above are obtained by using a semiclassical approximation [45], which consists of factoring joint operator moments $\langle a\sigma \rangle \rightarrow \langle a \rangle \langle \sigma \rangle$. Thereby, the cavity field is described by a complex amplitude $\langle a \rangle = \alpha$ rather than a quantum mechanical operator.

The EIT-like phenomenon in this system is observed when the Rabi frequency of the cavity field $g\langle a \rangle_{\text{max}}$ is large compared to the Rabi frequency of the probe field, $\varepsilon_c \ll g\langle a \rangle_{\text{max}}$, and also when $\gamma_{eg} \ll \kappa$. The average $\langle a \rangle_{\text{max}} = \varepsilon_c/(\Delta_c - i\kappa)$ is the maximum value of $\langle a \rangle$ in the absence of atoms ($g = 0$). As we have seen in the previous section, the optical response of the atom-cavity medium is proportional to the expectation value of the cavity field $\langle a \rangle$, once the cavity mode is pumped weakly by the probe field. Then we represent the probe response as an
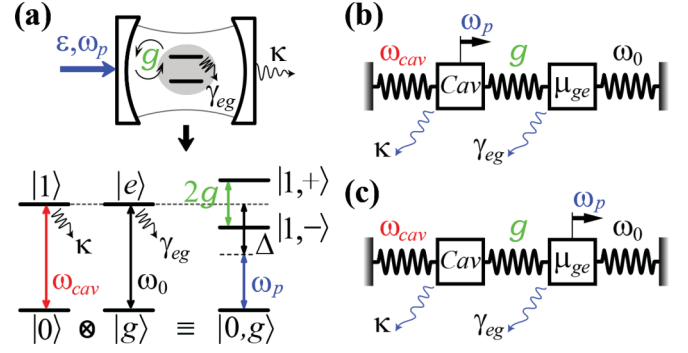

FIG. 4. (Color online) (a) (Top) Single two-level atom with resonance frequency ω_0 and atomic polarization decay rate γ_{eg}, interacting with a single mode of an optical resonator with frequency ω_{cav} and cavity decay rate κ. The atom-field dipole coupling is described by the vacuum Rabi frequency $2g$. A classical probe field with frequency ω_p and strength ε pumps either the cavity or the atom. (Bottom) First doublet of dressed states of the Jaynes-Cummings ladder as a result of the coupling between the bare cavity ($|0\rangle,|1\rangle$) and the bare atom ($|g\rangle,|e\rangle$). Panels (b) and (c) show the atom-field classical analogs for the driven cavity and driven atom cases, respectively.

atom-cavity reduced susceptibility $\tilde{\chi}_{AC}(\omega_p) = \langle a \rangle$. The real part of $\tilde{\chi}_{AC}$ is related to the absorption spectrum of the system and its imaginary part to the phase of the outgoing light field of the cavity. In the steady state, $\dot{\rho} = 0$, the equations above give for the expectation value of the photon annihilation operator,

$$\langle a \rangle = \frac{-\varepsilon_c(\Delta_c - i\gamma_{eg})}{(\Delta_c - i\kappa)(\Delta_c - i\gamma_{eg}) + g^2\langle \sigma_z \rangle}. \quad (24)$$

If $\langle \sigma_z \rangle = -1$, $\langle a \rangle$ becomes identical to the reduced mechanical susceptibility $\tilde{\chi}_M(\omega_s) = \rho_{co}$; see Eq. (15). Mathematically, $\langle \sigma_z \rangle = -1$ is the limit to reach low atomic excitation, meaning that the probe field is so weak that we can consider only the zero- and one-photon states ($|0\rangle,|1\rangle$) of the cavity mode. As illustrated in Fig. 4(a), the atom-field system will be limited to the first splitting of the dressed states which forms the anharmonic Jaynes-Cummings ladder.

The atom-field classical analog for the driven cavity case is shown in Fig. 4(b) and each parameter is identified as in Table III. It is also interesting to make comparisons between the original EIT-Λ scheme and other quantum systems. In

TABLE III. Classical analog of EIT for different quantum systems using two mechanical coupled harmonic oscillators (2-MCHO). We present the analogs for the three-level atom in Λ configuration (EIT-Λ), two coupled cavity modes (EIT-CCM), and two-level atom-cavity systems for the driven-cavity (EIT-DC) and driven-atom (EIT-DA) cases.

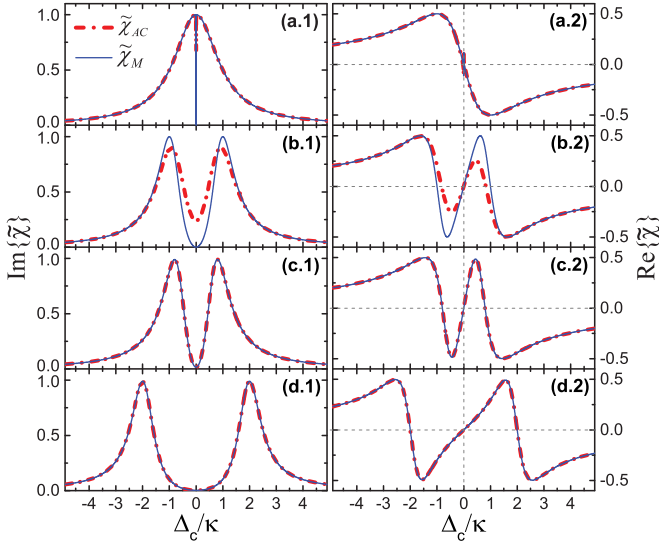| EIT-Λ	EIT-CCM	EIT-DC	EIT-DA	2-MCHO
ρ_{31}	$\langle a \rangle$	$\langle a \rangle$	$\langle \sigma_{ge} \rangle$	ρ_{co}
Δ_p	Δ_p	Δ_c	Δ_0	Δ_s
Ω_p	ε	ε_c	ε_0	Ω_s
Ω_c	λ	g	g	Ω_{12}
γ_{31}	κ_a	κ	γ_{eg}	γ_1
γ_2	κ_b	γ_{eg}	κ	γ_2

FIG. 5. (Color online) Imaginary and real parts of the reduced atom-cavity susceptibility $\tilde{\chi}_{AC}$ vs the normalized probe-cavity detuning Δ_c/κ for the two-level atom interacting with a single mode of a driven optical cavity in comparison with its mechanical analog $\tilde{\chi}_M$. The parameters are (a) $\varepsilon_c = 0.02\kappa$, $g = 0.02\kappa$, $\gamma_{eg} = 0.0$; (b) 0.5κ, 1.0κ, 0.0; (c) 0.02κ, 0.8κ, 0.01κ; and (d) 0.02κ, 2.0κ, 0.01κ. The classical results were obtained using the same set of parameters following the analog depicted in Table III.

this case, the cavity makes the role of the atomic transition $|1\rangle \leftrightarrow |3\rangle$ and the atom represents the transition $|2\rangle \leftrightarrow |3\rangle$; see Figs. 1(a) and 1(c).

Figure 5 shows the imaginary and real parts of the reduced susceptibility $\tilde{\chi}_{AC}(\omega_p)$ vs the normalized probe-cavity detuning Δ_c/κ for a different set of parameters in comparison with its classical analog $\tilde{\chi}_M(\omega_s)$. The full quantum atom-cavity description is solved for the steady state of ρ following the method presented in Ref. [46], where the cavity-field Fock basis is truncated according to the probe strength.

In Figs. 5(a) and 5(b) the EIT-like condition $\varepsilon_c \ll g\langle a\rangle_{\max}$ is not deeply satisfied, showing that the intracavity dark state $\langle a\rangle = 0$ for $\Delta_c = 0$ is not observed, differently for its classical counterpart once $\gamma_{eg} \equiv \gamma_2 = 0$; see Sec. 2 of the Appendix. When such condition is fulfilled the results show perfect agreement even for nonvanishing γ_{eg}, like in Figs. 5(c) and 5(d), since $\gamma_{eg} \ll \kappa$.

As we have mentioned, the condition $\langle \sigma_z \rangle = -1$ in Eq. (24) means the atom-cavity field can be described by the first doublets of dressed states of the Jaynes-Cummings ladder [see Fig. 4(a)], regardless the atom-cavity system being considered in the strong coupling regime $g \gg (\gamma_{eg}, \kappa)$, like in Fig. 5(d). Thus, the quantum atom-field correlations can be completely neglected, and then the atom and cavity field can be treated in the same footing as harmonic oscillators. In Ref. [47] the authors used the full classical result, given by Eq. (24), to analyze experimentally the measurement of antiresonances in a strongly coupled atom-cavity system by using heterodyne detection.

The aspects of EIT-like phenomenon regarding the spectrum of absorption obtained from the imaginary part of $\langle a\rangle$ can also be observed through the calculation of cavity

transmission. It is provided by the average photon number $\langle a^\dagger a\rangle$. Once we have the classical analog for $\langle a\rangle \equiv \rho_{co}$, one can see readily that $\langle a^\dagger a\rangle \equiv \rho_{co}^* \rho_{co}$.

For the driven atom case, the probe field with strength ε_0 pumps the atom instead of the cavity mode. For this system, the time-independent Hamiltonian in a rotating frame reads

$$H = \Delta_0 \sigma_{ee} + \Delta_c a^\dagger a + g(a\sigma_{eg} + a^\dagger \sigma_{ge}) + \varepsilon_0(\sigma_{eg} + \sigma_{ge}). \tag{25}$$

As before, we consider atom and cavity on resonance $\omega_0 = \omega_{\text{cav}}$; then $\Delta_c = \Delta_0$, where $\Delta_0 = \omega_0 - \omega_p$ is the probe-atom detuning. Once the probe field couples directly to the atom, the probe absorption is related to the density matrix element $\rho_{eg} = \langle \sigma_{ge}\rangle$, in analogy with ρ_{31} in Eq. (5). Then, the atom-cavity reduced susceptibility is represented by $\tilde{\chi}_{AC}(\omega_p) = \langle \sigma_{ge}\rangle$. Using the master equation (22) to obtain the time evolution for the atomic and field operators, we solve for the expectation value of the lowering atomic operator in the steady state,

$$\langle \sigma_{ge}\rangle = \frac{\varepsilon_0\langle \sigma_z\rangle(\Delta_0 - i\kappa)}{(\Delta_0 - i\gamma_{eg})(\Delta_0 - i\kappa) + g^2\langle \sigma_z\rangle}, \tag{26}$$

which is also identical to the mechanical reduced susceptibility $\tilde{\chi}_M = \rho_{co}$ for $\langle \sigma_z\rangle = -1$. Note that Eq. (24) can be recovered from Eq. (26) by changing $\gamma_{eg} \leftrightarrow \kappa$. Thus, the first EIT-like condition $\varepsilon_0 \ll g\langle a\rangle_{\max}$ remains the same and the second is now switched to $\kappa \ll \gamma_{eg}$. The classical analog for this system is illustrated in Fig. 4(d) and each atom-cavity parameter is identified classically in Table III.

Differently from Figs. 5(a) and 5(b), the dark state is observed in the driven atom for both classical and quantum responses. Like in the original EIT configuration presented in Fig. 2, the maximum absorption peaks in the quantum system decreases when the condition $\varepsilon_0 \ll g\langle a\rangle_{\max}$ is not deeply satisfied, meaning that the approximation $\langle \sigma_z\rangle = -1$ is not valid.

The dissipative rates γ_{eg} and κ for the driven-cavity ($\gamma_{eg} \ll \kappa$) and driven-atom ($\kappa \ll \gamma_{eg}$) cases, respectively, make the role of the nonradiative atomic dephasing rate of state $|2\rangle$, γ_2, in the EIT system. If those parameters are relatively large, the intracavity dark state will be no longer perfect [3].

The next sections are dedicated to showing the classical analog for atomic systems with more than three levels of energy using three coupled harmonic oscillators.

III. CLASSICAL ANALOG OF EIT IN DIFFERENT PHYSICAL SYSTEMS USING THREE COUPLED HARMONIC OSCILLATORS

Now we show how to represent mechanically the EIT-related phenomena observed in four-level atoms in the inverted-Y, tripod, and CEIT configurations. As we are adding an atomic allowed transition, coupled by a laser field, to the original atomic three-level EIT system, we have to add their classical equivalent in the mechanical system. Then, the mechanical configuration is composed by three coupled harmonic oscillators as shown in Fig. 6.

Hereafter we follow the same reasoning and notation used for the two coupled oscillators described previously. Considering the general case, where each particle is driven by a coherent force $F_{js}(t) = F_j e^{-i(\omega_s t + \phi_s)} + \text{c.c.}$ ($j = 1, 2, 3$) and
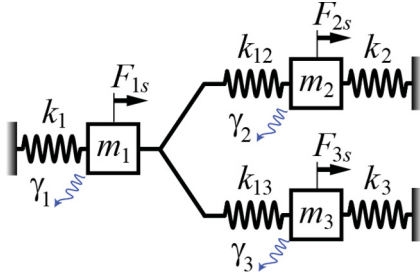
FIG. 6. (Color online) Mechanical model composed of three coupled damped harmonic oscillators used to reproduce the EIT-related phenomenology observed in multilevel atomic systems. It consists of three masses m_1, m_2, and m_3 attached to five springs with constant springs k_1, k_2, k_3 for the outside springs and k_{12}, k_{13} for the coupling springs. For the general case, a driving force $F_{js}(t)$ of frequency ω_s acts on mass m_j and the damping constant of the jth harmonic oscillator is represented by γ_j ($j = 1, 2, 3$).
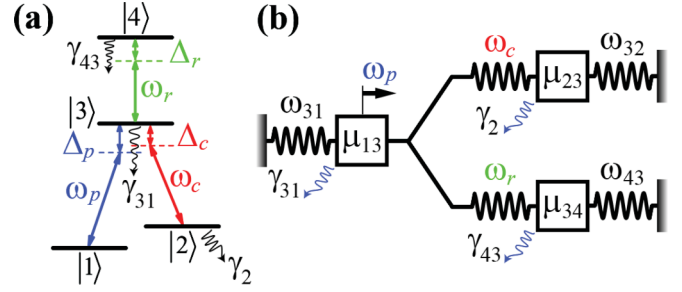

FIG. 7. (Color online) (a) Schematic energy level diagram of a four-level atom in the inverted-Y configuration, showing three classical electromagnetic fields, probe (ω_p), control (ω_c), and pump (ω_r), coupling the transitions $|1\rangle \leftrightarrow |3\rangle$, $|2\rangle \leftrightarrow |3\rangle$, and $|3\rangle \leftrightarrow |4\rangle$, respectively, and their corresponding detunings. The atomic decay rates are represented by $\gamma_{31} = \Gamma_{31} + \Gamma_{32} + \gamma_3$, $\gamma_{43} = \Gamma_{43} + \gamma_4$, and γ_2. The classical analog shown in (b) consists of only one force acting on mass m_1, meaning that $F_{2s} = F_{3s} = 0$ in Fig. 6.

assuming the solutions $x_j = N_j e^{-i\omega_s t} + $ c.c., the equations of motion on the three masses give rise to the equations

$$\left(-\omega_s^2 + \omega_1^2 - 2i\gamma_1\omega_s\right)N_1 - \omega_{12}^2 N_2 - \omega_{13}^2 N_3 = \frac{F_1}{m}e^{-i\phi_1},$$

(27a)

$$\left(-\omega_s^2 + \omega_2^2 - 2i\gamma_2\omega_s\right)N_2 - \omega_{12}^2 N_1 = \frac{F_2}{m}e^{-i\phi_2},$$

(27b)

$$\left(-\omega_s^2 + \omega_3^2 - 2i\gamma_3\omega_s\right)N_3 - \omega_{13}^2 N_1 = \frac{F_3}{m}e^{-i\phi_3},$$

(27c)

where $\omega_1^2 = (k_1 + k_{12} + k_{13})/m$, $\omega_2^2 = (k_2 + k_{12})/m$, $\omega_3^2 = (k_3 + k_{13})/m$, $\omega_{12}^2 = k_{12}/m$, $\omega_{13}^2 = k_{13}/m$, and ϕ_j ($j = 1, 2, 3$) are the respective phases. As before, we consider identical masses $m_1 = m_2 = m_3 = m$ and frequencies ω_j ($j = 1, 2, 3$) near to ω_s, implying that the approximations $\omega_j^2 - \omega_s^2 \approx 2\omega_j(\omega_j - \omega_s)$ and $\gamma_j\omega_s \approx \gamma_j\omega_j$ can be used and the corresponding detunings $\Delta_j = \omega_j - \omega_s$ properly defined. As before, we have omitted the complex conjugate solution (c.c.) for simplicity.

The mechanical representation of the atomic systems we are about to show are more complicated owing to the amount of dipole transitions and coupling fields. Depending on the atomic configuration, we choose which particle or particles in the classical system are driven by the corresponding forces $F_{js}(t)$.

The collective motion of the system for the configuration presented in Fig. 6 is described by three normal modes, owing to the addition of the third mass. Considering the simple case, where $k_i = k$ ($i = 1, 2, 3$) and $k_{1j} = k_\alpha$, with $\omega_{1j}^2 = \omega^2 = k_\alpha/m$ ($j = 2, 3$), the resonance frequencies are $\omega_0 = \sqrt{k/m}$, $\omega_+ = \sqrt{\omega_0^2 + \omega^2}$, and $\omega_- = \sqrt{\omega_0^2 + 3\omega^2}$, which are the frequencies of the normal modes $NM_{(0)}$, $NM_{(+)}$, and $NM_{(-)}$, respectively. The modes $NM_{(0)}$ and $NM_{(-)}$ are similar to the two normal modes described in Sec. II A. In $NM_{(0)}$ the three masses move in phase, while in $NM_{(-)}$, m_1 moves oppositely to m_2 and m_3. In the third mode, $NM_{(+)}$,

m_1 stays stationary, while m_2 and m_3 oscillate harmonically exactly out of phase with each other. The analysis performed in Sec. 2 of the Appendix can be extended to the present case by defining the normal coordinates X_0, X_+, and X_-, which are proportional to $x_1 + x_2 + x_3$, $x_2 - x_3$, and $x_1 - x_2 - x_3$, respectively, meaning that any arbitrary motion of the system is a superposition of those three normal modes. The classical dark state is defined according to the EIT-like conditions for each system.

A. EIT in four-level atoms in the inverted-Y configuration

The effect of two or more electromagnetic fields interacting with multilevel atomic systems has been extensively explored theoretically and experimentally in recent years [48]. The absorption spectrum of a variety of four-level atomic systems exposed to three laser fields is characterized by a double dark resonance. This effect is named as double EIT.

The four-level atom in the inverted-Y configuration can be seen as a three-level atom in Λ configuration, composed by the states $|1\rangle$, $|2\rangle$, and $|3\rangle$, plus a second excited state $|4\rangle$, as shown in Fig. 7(a). Transitions $|1\rangle \leftrightarrow |3\rangle$ and $|2\rangle \leftrightarrow |3\rangle$ interact with the probe and control fields as in the usual three-level Λ type. A third coupling field of frequency ω_r and Rabi frequency $2\Omega_r$, named as pumping field, couples the transition $|3\rangle \leftrightarrow |4\rangle$.

By introducing the dipole and RWAs, the time-independent Hamiltonian for this system can be written as

$$H = -\Delta_p\sigma_{11} - \Delta_c\sigma_{22} - \Delta_r\sigma_{44} - \Omega_p(\sigma_{13} + \sigma_{31})$$
$$- \Omega_c(\sigma_{23} + \sigma_{32}) - \Omega_r(\sigma_{43} + \sigma_{34}),$$

(28)

where the detunings are given by $\Delta_p = \omega_{31} - \omega_p$, $\Delta_c = \omega_{32} - \omega_c$, and $\Delta_r = \omega_{43} - \omega_r$. Its dynamics is obtained numerically by solving the master equation for the atomic density operator,

$$\dot{\rho} = -i[H, \rho] + \sum_{m=1,2} \Gamma_{3m}(2\sigma_{m3}\rho\sigma_{3m} - \sigma_{33}\rho - \rho\sigma_{33})$$

$$+ \Gamma_{43}(2\sigma_{34}\rho\sigma_{43} - \sigma_{44}\rho - \rho\sigma_{44})$$

$$+ \sum_{n=2,3,4} \gamma_n(2\sigma_{nn}\rho\sigma_{nn} - \sigma_{nn}\rho - \rho\sigma_{nn}),$$

(29)

with the polarization decay rate Γ_{43} and nonradiative atomic dephasing rate γ_4, accounting for the additional state $|4\rangle$.

The information about absorption and dispersion of the probe field in the four-level atomic medium is obtained through the reduced electric susceptibility $\tilde{\chi}_e(\omega_p) = \rho_{31}(\omega_p)$, in analogy with previous definitions. For the inverted-Y system we also used the weak probe field approximation, $\Omega_p \ll (\Omega_c, \Omega_r)$, implying that almost all the atomic population is in the ground state $\rho_{11} \approx 1$. From the full density-matrix equations of motion and assuming that the values of ρ_{43} and ρ_{23} are approximately zero [48], we solved for the steady state of ρ to find

$$\rho_{31}(\omega_p) = \frac{\Omega_p(\delta_2 - i\gamma_2)(\delta_4 - i\gamma_{43})}{\Upsilon_Q - \Omega_c^2(\delta_4 - i\gamma_{43}) - \Omega_r^2(\delta_2 - i\gamma_2)}, \quad (30)$$

where $\Upsilon_Q = (\Delta_p - i\gamma_{31})(\delta_2 - i\gamma_2)(\delta_4 - i\gamma_{43})$, $\gamma_{31} = \Gamma_{31} + \Gamma_{32} + \gamma_3$, and $\gamma_{43} = \Gamma_{43} + \gamma_4$. Here we introduced the two-photon detunings $\delta_2 = \Delta_p - \Delta_c$ and $\delta_4 = \Delta_p - \Delta_r$. Note that when $\Omega_r = 0$, Eq. (30) reduces to Eq. (8) for the three-level EIT-Λ configuration.

The classical analog to demonstrate double EIT in four-level atoms in the inverted-Y configuration was proposed by Serna *et al.* [12]. They used a mechanical system composed of three coupled harmonic oscillators and also an electric analog composed by three coupled RLC circuits. Here we used the same configuration as in Ref. [12] in order to identify an one-to-one correspondence between the classical and quantum dynamic variables for this system.

Its corresponding reduced mechanical susceptibility $\tilde{\chi}_M(\omega_s) = \rho_{co}(\omega_s)$ is obtained from Eqs. (27) by setting $F_{2s} = F_{3s} = 0$ and solving for the displacement of particle 1 for $\phi_1 = 0$,

$$\rho_{co}(\omega_s) = \frac{\Omega_s(\Delta_2 - i\gamma_2)(\Delta_3 - i\gamma_3)}{\Upsilon_C - \Omega_{12}^2(\Delta_3 - i\gamma_3) - \Omega_{13}^2(\Delta_2 - i\gamma_2)}, \quad (31)$$

where $\Upsilon_C = (\Delta_1 - i\gamma_1)(\Delta_2 - i\gamma_2)(\Delta_3 - i\gamma_3)$, the coupling rates $\Omega_{12} = \omega_{12}^2/2\sqrt{\omega_1\omega_2}$, $\Omega_{13} = \omega_{13}^2/2\sqrt{\omega_1\omega_3}$, and the pumping rate $\Omega_s = \sqrt{F_1^2/2m\omega_1}$. As we have discussed in Sec. II A the coupling-field detunings Δ_c and Δ_r in Eq. (30) can be reproduced readily in the classical system by setting $\Delta_1 = \Delta_s$, $\Delta_2 = \Delta_s - \Delta_{21}$, and $\Delta_3 = \Delta_s - \Delta_{31}$, where Δ_{21} and Δ_{31} account for the detuning between the frequencies of the oscillators 2-1 and 3-1, respectively. For perfect resonances $\Delta_c = \Delta_r = 0$, the classical detunings are reduced to $\Delta_1 = \Delta_2 = \Delta_3 = \Delta_s$. Note that even for $k_2 = k_3$ we have $\omega_2 \neq \omega_3$ so that, for the resonance case the analog is complete by adjusting the detunings to be identical through k_1, k_{12}, and k_{13}.

Comparing $\rho_{31}(\omega_p)$, Eq. (30), and $\rho_{co}(\omega_s)$, Eq. (31), we identify classically each parameter of the atomic system as in Table IV. The classical analog is illustrated in Fig. 7(b). As shown before, each atomic dipole-allowed transition corresponds to a harmonic oscillator in the mechanical system. Then the addition of state $|4\rangle$ and the coupling field of frequency ω_r imply the addition of one more harmonic oscillator (m_3) to account for the atomic transition $|3\rangle \leftrightarrow |4\rangle$ and a second coupling spring (k_{13}) to communicate energy to the pumped oscillator m_1.

TABLE IV. Classical analog of EIT-like for the four-level atom in an inverted-Y configuration (EIT-4Y) using three mechanical coupled harmonic oscillators (3-MCHO).

EIT-4Y (ρ_{31})	3-MCHO (ρ_{co})
Δ_p	Δ_1
δ_2	Δ_2
δ_4	Δ_3
Ω_p	Ω_s
Ω_c	Ω_{12}
Ω_r	Ω_{13}
γ_{31}	γ_1
γ_2	γ_2
γ_{43}	γ_3

The imaginary and real parts of the reduced electric susceptibility $\tilde{\chi}_e(\omega_p)$ are depicted in Fig. 8 as a function of the normalized probe-atom detuning Δ_p/γ_{31} in comparison with its classical counterpart $\tilde{\chi}_M(\omega_s)$. Figures 8(a) and 8(b) show disagreement between the results, meaning that the condition $\Omega_p \ll (\Omega_c, \Omega_r)$ is not deeply satisfied and part of the atomic population is not in the ground state $|1\rangle$. In Figs. 8(c) and 8(d) the condition is satisfied, with classical and quantum results showing excellent agreement. The classical dark state in this case is also produced when oscillator 1 stays stationary while oscillators 2 and 3 oscillate harmonically. Note that when $\omega_s = \omega_1 = \sqrt{(k_1 + k_{12} + k_{13})/m}$ the system is pumped in the range between the normal frequencies ω_0 and ω_-, which is a
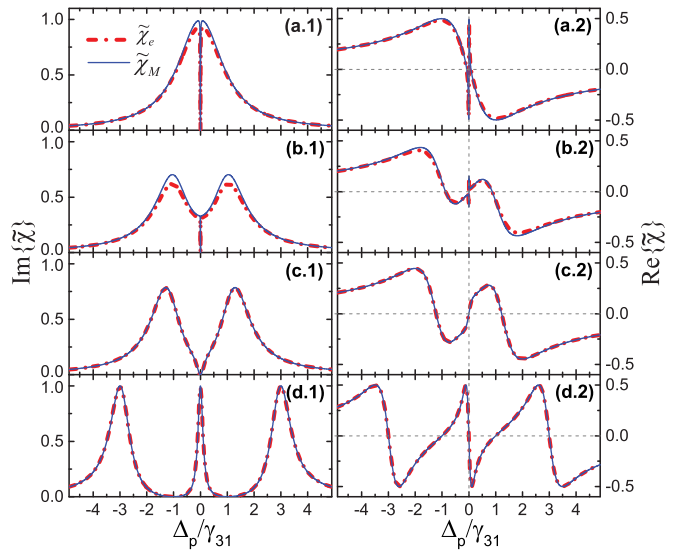

FIG. 8. (Color online) Imaginary and real parts of the reduced electric susceptibility ($\tilde{\chi}_e$) vs normalized probe-atom detuning Δ_p/γ_{31} for the four-level atom in a inverted-Y configuration in comparison with its classical counterpart ($\tilde{\chi}_M$) obtained using three coupled harmonic oscillators. The parameters are $\Omega_p = 0.02\gamma_{31}$, $\Gamma_{43} = 0.5\gamma_{31}$, $\gamma_2 = 0.0$; (a) $\Omega_c = \Omega_r = 0.08\gamma_{31}$, (b) $\Omega_c = 0.08\gamma_{31}$, $\Omega_r = 1.0\gamma_{31}$; (c) $\Omega_c = 0.8\gamma_{31}$, $\Omega_r = 1.0\gamma_{31}$; and (d) $\Omega_c = \Omega_r = 2.0\gamma_{31}$. The coupling-field detunings Δ_c, Δ_r are zero in (a)–(c); in (d) $\Delta_c = 1.0\gamma_{31}$, $\Delta_r = -1.0\gamma_{31}$. For the classical system we use the same set of parameters following the analog presented in Table IV.
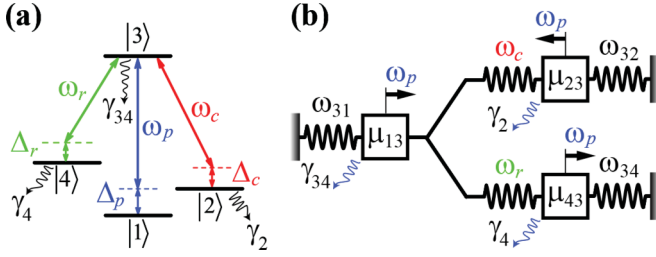
FIG. 9. (Color online) (a) Schematic energy level diagram of a four-level atom in a tripod configuration, showing three classical electromagnetic fields, probe (ω_p), control (ω_c), and pump (ω_r), coupling the transitions $|1\rangle \leftrightarrow |3\rangle$, $|2\rangle \leftrightarrow |3\rangle$, and $|3\rangle \leftrightarrow |4\rangle$, respectively, and their corresponding detunings. The atomic decay rates are represented by $\gamma_{34} = \Gamma_{31} + \Gamma_{32} + \Gamma_{34} + \gamma_3$, γ_2, and γ_4. The classical analog is obtained considering a force acting in each harmonic oscillator with phases $\phi_1 = \phi_3 = 0$ and $\phi_2 = \pi$, as shown in (b).

region of high probability of interference between the normal modes $NM_{(0)}$ and $NM_{(-)}$. Once $x_1 = 0$, it is featured by zero absorption power of oscillator 1, which is equivalent to $\tilde{\chi}_M = 0$ for zero detuning.

Figure 8(d) shows that a third resonance peak appears as a consequence of making the coupling-atom detunings Δ_c and Δ_r different from zero. If we set $\Omega_c = \Omega_r$, the peaks become symmetric, giving rise to two transmission windows, which characterizes double EIT. By manipulating the parameters of the system, we can control the two EIT dips from a narrow to a wider splitting of the Autler-Townes doublets. We see that all these resonant features can be reproduced with the mechanism of classical interference of the normal modes of the three coupled harmonic oscillators in the displacement of oscillator 1.

B. EIT in four-level atom in a tripod configuration

The four-level atom in a tripod configuration is also based on a three-level EIT system and it is promising for many applications, ranging from the realization of polarization quantum phase gates to quantum information processes [49–52]. Different from the inverted-Y configuration, here the atomic level $|4\rangle$ is a ground state; see Fig. 9(a). The time-independent Hamiltonian is essentially the same as Eq. (28) and the master equation is slightly modified as

$$\dot{\rho} = -i[H,\rho] + \sum_{m=1,2,4} \Gamma_{3m}(2\sigma_{m3}\rho\sigma_{3m} - \sigma_{33}\rho - \rho\sigma_{33})$$
$$+ \sum_{n=2,3,4} \gamma_n(2\sigma_{nn}\rho\sigma_{nn} - \sigma_{nn}\rho - \rho\sigma_{nn}), \quad (32)$$

where we introduce the polarization decay rate Γ_{34} of the excited level $|3\rangle$ to the level $|4\rangle$.

In the same way as in the inverted-Y configuration the response of the probe field is given by the reduced electric susceptibility $\tilde{\chi}_e = \rho_{31}$. Solving for ρ_{31} and considering the
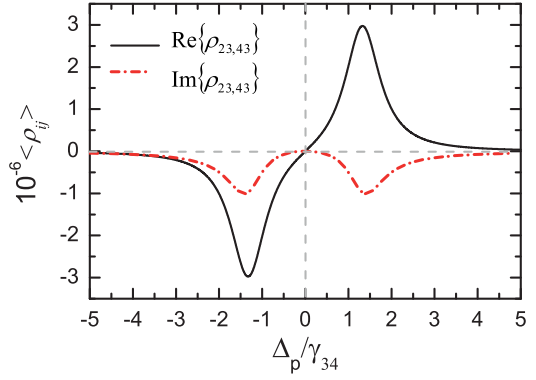

FIG. 10. (Color online) Imaginary and real parts of ρ_{23} and ρ_{43} vs the normalized probe-atom detuning Δ_p/γ_{34} for perfect atom-field resonances $\Delta_c = \Delta_r = 0$, using the parameters $\Omega_p = 0.002\gamma_{34}$, $\Omega_c = \Omega_r = 1.0\gamma_{34}$, and $\gamma_2 = \gamma_4 = 0$.

limit of low atomic excitation $\rho_{11} \approx 1$, we have

$$\rho_{31} = \frac{\Omega_p(\Delta_p - i\gamma_2)(\Delta_p - i\gamma_4) - \Omega_p\Omega_c\Upsilon_{23} - \Omega_p\Omega_r\Upsilon_{43}}{\Upsilon_Q - \Omega_c^2(\Delta_p - i\gamma_4) - \Omega_r^2(\Delta_p - i\gamma_2)},$$
$$(33)$$

where $\Upsilon_{23} = (\Delta_p - i\gamma_4)\rho_{23}$, $\Upsilon_{43} = (\Delta_p - i\gamma_2)\rho_{43}$, and $\Upsilon_Q = (\Delta_p - i\gamma_{34})(\Delta_p - i\gamma_2)(\Delta_p - i\gamma_4)$, with $\gamma_{34} = \Gamma_{31} + \Gamma_{32} + \Gamma_{34} + \gamma_3$.

The real and imaginary parts of the nondiagonal density matrix element ρ_{23} are identical to those for ρ_{43}, as shown in Fig. 10. Despite their small values, they are not neglected here, like in the inverted-Y configuration. Note that the real parts of $\rho_{23,43}$ change their signal with Δ_p, while the signal of the imaginary parts are kept the same. These details are essential to obtain the correct classical analog for the atomic tripod configuration.

If we consider $\Omega_r = 0$ in Eq. (33), we end up with

$$\rho_{31} = \frac{\Omega_p(\Delta_p - i\gamma_2) - \Omega_p\Omega_c\rho_{23}}{(\Delta_p - i\gamma_{34})(\Delta_p - i\gamma_2) - \Omega_c^2}. \quad (34)$$

Apart from the dimensionless term ρ_{23}, the equation above has the same form of a mechanical model composed of two harmonic oscillators with two forces acting on particles 1 and 2 out of phase by π. In Eqs. (27) we would have $F_2 = -F_1$ for $k_{13} = 0$, or $F_3 = -F_1$ for $k_{12} = 0$, once the same is observed for $\Omega_c = 0$. Then, as a first suggestion, one could propose the classical analog for the atomic tripod configuration by considering the forces F_{2s} and F_{3s} out of phase with F_{1s} by π, i.e., $\phi_1 = 0$ and $\phi_2 = \phi_3 = \pi$. However, Fig. 10 shows that the real parts of $\rho_{23,43}$ are in phase with their corresponding imaginary parts for $\Delta_p < 0$ and out of phase by π for $\Delta_p > 0$. As additional transitions, ρ_{23} and ρ_{43}, represent additional harmonic oscillators, we reproduce this effect by assuming only the force acting on particle 2 out of phase by π with the force applied on particle 1, meaning that $F_2 = -F_1$ and $F_3 = F_1$. This classical model mimics the EIT features presented by the tripod configuration in very good agreement.

Taking into account the considerations above, the reduced mechanical susceptibility is obtained from Eqs. (27) for the

TABLE V. Classical analog of EIT-like phenomenon in a four-level atom in a tripod configuration (EIT-tripod) using three mechanical coupled harmonic oscillators considering the forces acting on the three particles as $F_2 = -F_1$ and $F_3 = F_1$ for our model (3CO) and $F_2 = F_3$ and $F_1 = 0$ for Huang's model (3CO-H) [13].

EIT-tripod (ρ_{31})	3CO (ρ_{co})	3CO-H (ρ_{co}^H)
Δ_p	Δ_s	Δ_s
Ω_p	Ω_s	Ω_s
Ω_c	Ω_{12}	Ω_{12}, Ω_{13}
Ω_r	Ω_{13}	Ω_{12}, Ω_{13}
γ_{34}	γ_1	γ_1
γ_2	γ_2	γ_1, γ_2
γ_4	γ_3	γ_3
Υ_{23}	Υ_3	
$-\Upsilon_{43}$	Υ_2	

displacement of oscillator 1 as

$$\rho_{co} = \frac{\Omega_s^{(1)}(\Delta_2 - i\gamma_2)(\Delta_3 - i\gamma_3) - \Omega_s^{(2)}\Omega_{12}\Upsilon_3 + \Omega_s^{(3)}\Omega_{13}\Upsilon_2}{\Upsilon_C - \Omega_{12}^2(\Delta_3 - i\gamma_3) - \Omega_{13}^2(\Delta_2 - i\gamma_2)},$$
(35)

where $\Upsilon_3 = \Delta_3 - i\gamma_3$, $\Upsilon_2 = \Delta_2 - i\gamma_2$, $\Upsilon_C = (\Delta_1 - i\gamma_1)(\Delta_2 - i\gamma_2)(\Delta_3 - i\gamma_3)$, $\Omega_{12} = \omega_{12}^2/2\sqrt{\omega_1\omega_2}$, and $\Omega_{13} = \omega_{13}^2/2\sqrt{\omega_1\omega_3}$. The mechanical pumping rates are given by $\Omega_s^{(j)} = \sqrt{F_j^2/(2m\omega_j)}$ and they are related to the force F_j acting on the jth oscillator, $j = 1,2,3$.

Once there is only one probe field applied to the atomic system with Rabi frequency Ω_p, Eq. (33), the classical pumping rates have to be the same, i.e., $\Omega_s^{(j)} = \Omega_s$. Consequently, $\omega_1 = \omega_2 = \omega_3$, implying that $k_2 = k_1 + k_{13}$ and $k_3 = k_1 + k_{12}$. This also conducts to $\Delta_1 = \Delta_2 = \Delta_3 = \Delta_s$. Considering all these conditions, Eq. (35) becomes identical to Eq. (33) for the atomic system. The classical analog for each parameter is depicted in Table V and illustrated in Fig. 9(b).

Huang *et al.* [13] proposed recently a classical analog for the atomic tripod configuration, considering $F_1 = 0$ and $F_2 = F_3$ in Eqs. (27). According to them their classical analog, or in our terms, their reduced mechanical susceptibility $\tilde{\chi}_M^H = \rho_{co}^H$ is obtained solving for the displacement of oscillators 2 or 3. Using these conditions and the same definitions above, we have

$$\rho_{co}^H = \frac{\Omega_s(\Delta_s - i\gamma_1)(\Delta_s - i\gamma_3) - \Omega_s\Omega_{13}^2 + \Omega_s\Omega_{12}\Omega_{13}}{\Upsilon_C - \Omega_{12}^2(\Delta_s - i\gamma_3) - \Omega_{13}^2(\Delta_s - i\gamma_2)}.$$
(36)

Comparing Eq. (36) with ρ_{31}, Eq. (33), we see that it is not possible to establish a one-to-one classical correspondence for the quantum variables $\Upsilon_{23} = (\Delta_p - i\gamma_4)\rho_{23}$ and $\Upsilon_{43} = (\Delta_p - i\gamma_2)\rho_{43}$. According to Eq. (36), we would have $\Omega_c\Upsilon_{23} \equiv \Omega_{13}^2$ and $-\Omega_r\Upsilon_{43} \equiv \Omega_{12}\Omega_{13}$. The classical analog for the other variables are shown in Table V. Note that we have two constraints for the classical variables in this case, $\gamma_1 = \gamma_2$ and $\Omega_{12} = \Omega_{13}$.

In Fig. 11 we plot the real and imaginary parts of the reduced electric susceptibility $\tilde{\chi}_e$ for the atomic system as a function of the normalized probe-atom detuning Δ_p/γ_{34} in comparison with its two classical counterparts $\tilde{\chi}_M$ and $\tilde{\chi}_M^H$, obtained from Eqs. (35) and (36), respectively. We consider the weak-
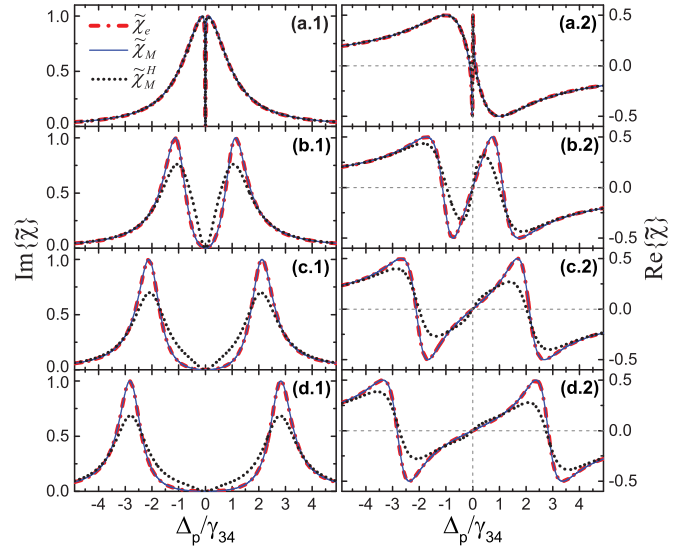

FIG. 11. (Color online) Imaginary and real parts of the reduced electric susceptibility $\tilde{\chi}_e$ vs normalized probe-atom detuning Δ_p/γ_{34} for the four-level atom in a tripod configuration in comparison with its classical counterparts $\tilde{\chi}_M$, Eq. (35), and $\tilde{\chi}_M^H$, Eq. (36), obtained using three coupled harmonic oscillators. The parameters are $\Omega_p = 0.002\gamma_{34}$, $\Delta_c = \Delta_r = 0$, $\gamma_2 = \gamma_4 = 0$ for different values of the Rabi frequencies of the coupling Ω_c and pumping Ω_r fields. We consider $\Omega_c = \Omega_r$ with values (a) $0.08\gamma_{34}$, (b) $0.8\gamma_{34}$, (c) $1.5\gamma_{34}$, and (d) $2.0\gamma_{34}$. For the classical models we obtain $\tilde{\chi}_M$ and $\tilde{\chi}_M^H$ using the same set of parameters following the analog presented in Table V.

probe limit $\Omega_p \ll (\Omega_c, \Omega_r)$, with $\Omega_p = 0.002\gamma_{34}$ for perfect coupling-field resonances $\Delta_c = \Delta_r = 0$ and $\gamma_2 = \gamma_4 = 0$. For all cases we consider $\Omega_c = \Omega_r$ owing the constraint obtained from Eq. (36), where $\Omega_{12} = \Omega_{13}$.

Figure 11(a) shows that both classical analogs reproduce the EIT features calculated for the atomic tripod system in very good agreement. When the Rabi frequencies of the coupling (Ω_c) and pumping (Ω_r) fields increase, Figs. 11(b)–11(d) show that only the mechanical susceptibility $\tilde{\chi}_M$, given by Eq. (35), reproduces satisfactorily the behavior of the atomic system.

Despite the impossibility of obtaining a one-to-one correspondence between classical and quantum variables, the classical analog proposed in Ref. [13], Eq. (36), exhibits a behavior similar to that of the tripod configuration, but total agreement is observed only for small values of Ω_{12}, Ω_{13}. If the EIT-like condition $\Omega_p \ll (\Omega_c, \Omega_r)$ is deeply satisfied, the analog proposed here shows perfect agreement for any set of parameters.

C. Cavity EIT

In Sec. II C we show the classical analog for a system consisting of a single two-level atom coupled to a single cavity mode. In this section we present for the first time the analog for the extended system considering a three-level atom placed inside an optical cavity. This system also exhibits EIT features being usually referred to as intracavity EIT or simply CEIT. The optical cavity enhances the main characteristics of EIT, regarding atomic coherence and interference, which may
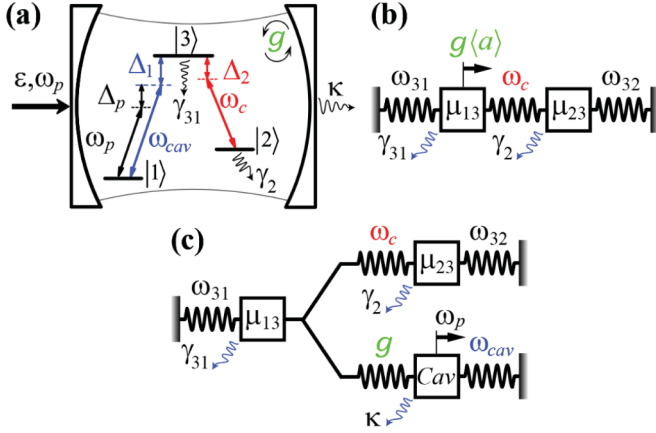
FIG. 12. (Color online) Three-level atom in a Λ configuration inside an optical resonator showing the quantum cavity field with frequency ω_{cav} and vacuum Rabi frequency $2g$ coupling the atomic transition $|1\rangle \leftrightarrow |3\rangle$. The control field with frequency ω_c couples the transition $|2\rangle \leftrightarrow |3\rangle$ and the probe field with frequency ω_p and strength ε drives the cavity mode. (b) Classical analog for $\langle\sigma_{13}\rangle$ given by Eq. (39) corresponding to two coupled harmonic oscillators pumped by the Rabi frequency of the cavity field $g\langle a\rangle$. (c) Classical analog for each parameter of the CEIT system.

be useful for a variety of fundamental studies and practical applications [53–56].

The system is comprised of a single atom with three energy levels in Λ configuration, as in Fig. 1(a), coupled to a single electromagnetic mode of frequency ω_{cav} of an optical resonator; see Fig. 12(a). The cavity is driven by a coherent field (probe) of strength ε and frequency ω_p. The atomic transitions $|1\rangle \leftrightarrow |3\rangle$ (frequency ω_{31}) and $|2\rangle \leftrightarrow |3\rangle$ (frequency ω_{32}) are coupled by the cavity mode with vacuum Rabi frequency $2g$ and by a classical field (control) with frequency ω_c and Rabi frequency $2\Omega_c$, respectively. The time-independent Hamiltonian which describes the atom-field coupling in a rotating frame is given by

$$
H = -\Delta_p \sigma_{11} + (\Delta_1 - \Delta_2)\sigma_{22} + \Delta_1 \sigma_{33} + \Delta_p a^\dagger a
$$
$$
+ (ga\sigma_{31} + \Omega_c \sigma_{32} + \varepsilon a + \mathrm{H.c.}), \tag{37}
$$

where the detunings are $\Delta_p = \omega_{\mathrm{cav}} - \omega_p$, $\Delta_1 = \omega_{31} - \omega_{\mathrm{cav}}$, and $\Delta_2 = \omega_{32} - \omega_c$. The master equation for the atom-cavity density operator is the same as Eq. (22), where we have to consider the cavity-field decay rate κ, the polarization decay rates Γ_{3m} ($m = 1,2$) of the excited level $|3\rangle$ to the levels $|m\rangle$, and the nonradiative atomic dephasing rates γ_n ($n = 2,3$) of states $|n\rangle$.

Similarly to the standard two-level atom-cavity system (CQED), in the EIT-like condition $\Omega_c \gg g\langle a\rangle_{\max}$, with $\langle a\rangle_{\max} = \varepsilon/(\Delta_p - i\kappa)$, the CEIT system will be limited to the first splitting of the dressed states, Autler-Townes-like effect, separated by $2\sqrt{g^2 + \Omega_c^2}$. Additionally, there are the intracavity dark states which cause an empty-cavity-like transmission, not observed in the two-level CQED configuration. The CEIT dressed states also compose a kind of anharmonic Jaynes-Cummings ladder structure [56].

The probe response is given by the reduced atom-cavity susceptibility, which is represented by the expectation value

of the cavity field $\tilde{\chi}_{\mathrm{CEIT}}(\omega_p) = \langle a\rangle$. In the steady state $\dot{\rho} = 0$ and considering the low atomic excitation limit $\langle\sigma_{11}\rangle \approx 1$, we have

$$
\langle a\rangle = \frac{-\varepsilon(\delta_1 - i\gamma_{31})(\delta_2 - i\gamma_2) + \varepsilon\Omega_c^2}{\Upsilon_Q - \Omega_c^2(\Delta_p - i\kappa) - g^2(\delta_2 - i\gamma_2)}, \tag{38}
$$

where $\Upsilon_Q = (\delta_1 - i\gamma_{31})(\delta_2 - i\gamma_2)(\Delta_p - i\kappa)$, with $\gamma_{31} = \Gamma_{31} + \Gamma_{32} + \gamma_3$, $\delta_1 = \Delta_p - \Delta_1$, and $\delta_2 = \delta_1 - \Delta_2$.

Once the atom-cavity system consists of two atomic dipole-allowed transitions and one cavity mode, its classical analog is also modeled on three coupled harmonic oscillators. The analysis of the probe response for the tripod system, given by ρ_{31}, revealed that more than one mechanical force has to be taken into account in the mechanical configuration. For all other systems considered before, we see that the probe field is represented by a coherent force applied only on the harmonic oscillator corresponding to the respective atomic transition or cavity mode.

By inspection of the expectation value of σ_{13}, written as

$$
\langle\sigma_{13}\rangle = \frac{-g\langle a\rangle(\delta_2 - i\gamma_2)}{(\delta_1 - i\gamma_{31})(\delta_2 - i\gamma_2) - \Omega_c^2}, \tag{39}
$$

we see that it is basically the equation for two coupled harmonic oscillators pumped by the Rabi frequency of the cavity field $g\langle a\rangle$, as illustrated in Fig. 12(b). Thus, for the classical analog of CEIT we also consider only one force applied on the harmonic oscillator representing the cavity mode, which is driven by the probe field.

Then, the classical analog is obtained from Eqs. (27) considering $F_{1s} = F_{2s} = 0$. Solving for the displacement of particle 3 and considering $\phi_3 = \pi$, we find for the reduced mechanical susceptibility $\tilde{\chi}_M = \rho_{co}$,

$$
\rho_{co}(\omega_s) = \frac{-\Omega_s(\Delta_1 - i\gamma_1)(\Delta_2 - i\gamma_2) + \Omega_s\Omega_{12}^2}{\Upsilon_C - \Omega_{12}^2(\Delta_3 - i\gamma_3) - \Omega_{13}^2(\Delta_2 - i\gamma_2)}, \tag{40}
$$

where $\Upsilon_C = (\Delta_1 - i\gamma_1)(\Delta_2 - i\gamma_2)(\Delta_3 - i\gamma_3)$, $\Omega_{12} = \omega_{12}^2/2\sqrt{\omega_1\omega_2}$, $\Omega_{13} = \omega_{13}^2/2\sqrt{\omega_1\omega_3}$, and $\Omega_s = \sqrt{F_3^2/2m\omega_3}$. Note that Eqs. (38) and (40) are identical. The classical analog for each parameter of the CEIT system is shown in Table VI and illustrated in Fig. 12(c).

Figures 13 and 14 show the real and imaginary parts, respectively, of the reduced atom-cavity susceptibility $\tilde{\chi}_{\mathrm{CEIT}}$ vs

TABLE VI. Classical analog of EIT-like phenomenon for the CEIT system using three mechanical coupled harmonic oscillators (3-MCHO).

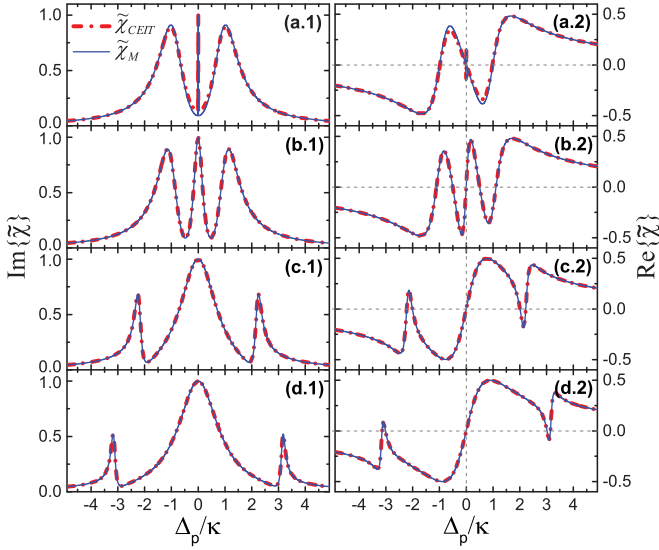| CEIT ($\langle a\rangle$)	3-MCHO (ρ_{co})
δ_1	Δ_1
δ_2	Δ_2
Δ_p	Δ_3
ε	Ω_s
Ω_c	Ω_{12}
g	Ω_{13}
γ_{31}	γ_1
γ_2	γ_2
κ	γ_3

FIG. 13. (Color online) Imaginary and real parts of the reduced atom-cavity electric susceptibility $\tilde{\chi}_{CEIT}$ vs the normalized probe-cavity detuning Δ_p/κ for the CEIT system in comparison with its classical counterpart $\tilde{\chi}_M$ for $\Omega_p = 0.02\kappa$, $g = 1.0\kappa$, $\gamma_{31} = 0.1\kappa$, $\gamma_2 = 0$, $\Delta_1 = \Delta_2 = 0$, and different values of the Rabi frequency of the control field (a) $\Omega_c = 0.02\kappa$, (b) 0.5κ, (c) 2.0κ, and (d) 3.0κ. For the classical system we use the same set of parameters following the analog presented in Table VI.

the normalized probe-cavity detuning Δ_p/κ for perfect atom-field resonances $\Delta_1 = \Delta_2 = 0$ in comparison with its classical counterpart $\tilde{\chi}_M$. The Rabi frequency of the probe field is set to be $\Omega_p = 0.02\kappa$ in Figs. 13, 14(c), and 14(d) and $\Omega_p = 0.5\kappa$ in Figs. 14(a) and 14(b), while the dissipation rates are fixed at $\gamma_{31} = 0.1\kappa$, $\gamma_2 = 0$. In Fig. 13 the vacuum Rabi frequency is fixed at $g = 1.0\kappa$ and the steady state of $\langle a \rangle$ is calculated for different values of the Rabi frequency of the control field Ω_c. In Fig. 14 we do the opposite, fixing $\Omega_c = 1.0\kappa$ and varying g.
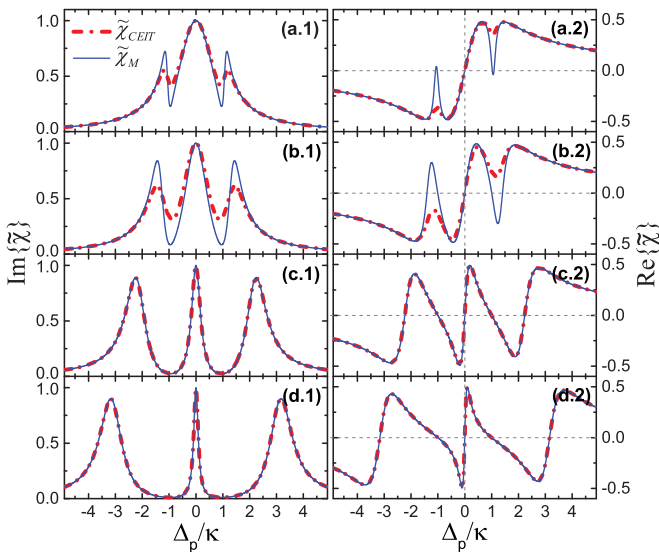

FIG. 14. (Color online) The same as in Fig. 13 for $\Omega_c = 1.0\kappa$, $\gamma_{31} = 0.1\kappa$, $\gamma_2 = 0$, $\Delta_1 = \Delta_2 = 0$, and (a) $\Omega_p = 0.5\kappa$, $g = 0.5\kappa$, (b) 0.5κ, 1.0κ, (c) 0.02κ, 2.0κ, and (d) 0.02κ, 3.0κ.
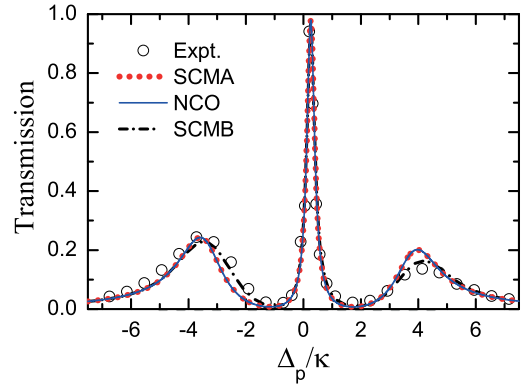

FIG. 15. (Color online) Experimental transmission spectrum (open circles) vs normalized probe-cavity detuning Δ_p/κ for the CEIT system reported in Ref. [27] for $N \approx 15$ atoms in comparison with a semiclassical model and the classical harmonic oscillators. The parameters used for the semiclassical theory, which considers 15 resting atoms (SCMA, red dotted line), are $\varepsilon = \sqrt{0.02}\kappa$, $g = 0.85\kappa$, $\Omega_c = 1.5\kappa$, $\gamma_{31} = 1.04\kappa$, $\gamma_2 = 0.001\kappa$, $\Delta_1 = -0.3\kappa$, and $\Delta_2 = 0$. For the mechanical system, solid blue line (NCO), we make use of the classical analog for N oscillators in Eq. (42) to calculate $\rho_{Nco}^* \rho_{Nco}$, using the same set of parameters according to Table VI and the analog for the atom-cavity detuning $\Delta_{13} = -0.3\gamma_3$. The black dash-dotted line is obtained from the same semiclassical theory as SCMA, but considering the atoms inside the cavity in movement (SCMB). This is performed by changing randomly the parameters g, Δ_1, and Δ_2 in an interval of values specified from experimental considerations.

Note that there is a small difference between the classical and quantum results in Fig. 13(a). If we increase the magnitude of Ω_p, the difference becomes more pronounced, as displayed in Figs. 14(a) and 14(b). In these cases the CEIT condition $\Omega_c \gg g\langle a \rangle_{max}$ is not deeply satisfied and $\langle \sigma_{11} \rangle \neq 1$. For all other set of parameters the results show perfect agreement.

The classical dark state, equivalent to the intracavity dark state of the CEIT system, is now observed when oscillator 3 is driven resonantly $\omega_s = \omega_3 = \sqrt{(k_3 + k_{13})/m}$. Note that this is exactly the resonance frequency ω_+ of the normal mode $NM_{(+)}$, where m_1 stays stationary while m_2 and m_3 oscillate harmonically out of phase with each other. Thus, the classical dark state is naturally identified as a peak in ω_3, meaning that the power transferred from the harmonic source to oscillator 3 is total and featured by $Im\{\tilde{\chi}_M\} = 1$ in Figs. 13 and 14 for zero detuning.

Figure 15 displays the transmission spectrum of CEIT obtained experimentally by Mücke *et al.* for 15 atoms, on average, trapped inside a high-finesse cavity [27], in comparison with a semiclassical and the classical analog models. As mentioned before, the semiclassical model is obtained from the semiclassical approximation $\langle a\sigma \rangle \rightarrow \langle a \rangle \langle \sigma \rangle$, where only the field is treated classically. It means that the quantized nature of the three-state atom is respected with $\langle a\sigma_{11} \rangle \neq \langle a \rangle$, differently from the full classical case given by Eq. (38). The red dotted line in Fig. 15, labeled SCMA, shows the semiclassical result for $N = 15$ resting atoms and the black dash-dotted line (SCMB) shows the same semiclassical model but considering atomic motion as in Ref. [27]. The parameters were adjusted in order to obtain the best fitting. The dephasing

rate of state $|2\rangle$ and the atom-cavity detuning, for example, were set to be $\gamma_2 = 0.001\kappa$ and $\Delta_1 = -0.3\kappa$, respectively, owing the decreasing in the transmission and the shifting of the central intracavity dark-state peak.

We can model mechanically N atoms by considering N pairs of harmonic oscillators, like in Fig. 12(b), coupling independently to oscillator 3, which represents the driven cavity mode. The dynamics of the three-level atom pumped by the Rabi frequency of the cavity can be obtained from the displacement of particle 1 in Eqs. (27). Substituting N_2 from Eq. (27b) in Eq. (27a), we have

$$N_1 = \frac{\Omega_{13}\tilde{N}_3(\Delta_2 - i\gamma_2)}{(\Delta_1 - i\gamma_1)(\Delta_2 - i\gamma_2) - \Omega_{12}^2}, \quad (41)$$

where $\tilde{N}_3 = \sqrt{\omega_3/\omega_1}N_3$. Note that Eq. (41) is the classical analog for $\langle\sigma_{13}\rangle$ given by Eq. (39). It represents the mechanical atom being pumped by the third harmonic oscillator with pumping rate $\Omega_{13}\tilde{N}_3$, in analogy to the Rabi frequency of the cavity field $g\langle a\rangle$ in the quantum model. Then, if we want to model mechanically N atoms independently coupled to a single cavity mode, we have to consider $N \times N_1$ in Eq. (27c). Thus, substituting Eq. (41) into Eq. (27c) for $\phi_3 = \pi$, we end up with

$$\rho_{Nco} = \frac{-\Omega_s(\Delta_1 - i\gamma_1)(\Delta_2 - i\gamma_2) + \Omega_s\Omega_{12}^2}{\Upsilon_C - \Omega_{12}^2(\Delta_3 - i\gamma_3) - N\Omega_{13}^2(\Delta_2 - i\gamma_2)}. \quad (42)$$

We see that the only difference between Eqs. (40) and (42) is to change the mechanical coupling rate Ω_{13} for the effective coupling $\Omega_{13}^{(\text{eff})} = \sqrt{N}\Omega_{13}$, where N is the number of pairs of harmonic oscillators as in Fig. 12(b). Then, to resemble the quantum mechanical average photon number $\langle a^\dagger a\rangle$, which provides the transmission spectrum depicted in Fig. 15, we have to calculate $\rho_{Nco}^*\rho_{Nco}$ from Eq. (42) for $N = 15$. As stated before the atom-cavity detuning can be modeled by setting $\Delta_3 = \Delta_s$ and $\Delta_1 = \Delta_s + \Delta_{13}$, where Δ_{13} accounts for the detuning of the resonant frequencies between oscillators 1–3.

Using the same set of parameters for the semiclassical model, following the analog depicted in Table VI, the full classical result is plotted in Fig. 15 (solid blue line), showing excellent agreement with the semiclassical model SCMA. It indicates that the experiment was performed by considering the CEIT conditions deeply, where $\langle\sigma_{11}\rangle \approx 1$, once the difference between the experimental data and the SCMA theory is solved by taking into account the movement of the atoms inside the cavity, which is corroborated by the SCMB model.

IV. CONCLUSIONS

In this work we showed that mechanical analogs can be obtained for atomic systems which present EIT-related phenomena, if they are considered deeply in the EIT-like conditions. In this case atoms and single cavity modes behave as oscillating dipoles and all dissipative and coherent atom-field processes can be reproduced with systems composed by coupled damped harmonic oscillators. The frequencies of the spectral lines of the atom are equivalent to the natural oscillation frequencies of the oscillators, showing that each atomic dipole allowed transition corresponds to a classical

harmonic damped oscillator. We also show that the classical dark state is caused by a destructive interference between the normal modes of the system in the displacement of the driven oscillator, and it is observed in analogous conditions with the dark state of the corresponding EIT system.

Through the concept of mechanical susceptibility, with its imaginary part corresponding to the power absorbed by the driven oscillator and its real part related to its amplitude, the classical models presented here describe correctly the action of the atom interacting with an electromagnetic field, reproducing the imaginary and real behavior of the electric susceptibility, respectively. Nevertheless, when the population of the atomic system is shared between its bare states ($\rho_{11} \neq 1$) or when anharmonic effects takes place, owing to the excitation of high-energy states, the classical models do not provide a detailed description of the phenomena the way the full quantum theory does. It would be interesting to introduce anharmonicities in the dynamics of the coupled oscillators in order to further explore the connection between these with quantum effects when the EIT-like conditions are not deeply prescribed.

Furthermore, the probe response of driven cavity modes and atom-cavity configurations provide a physical interpretation for the average photon annihilation operator $\langle a\rangle$, revealing that it can be directly related to the electric susceptibility of the system.

In conclusion, the fact that we can reproduce the phenomenology of EIT with classical harmonic oscillators does not mean EIT is a classical phenomenon. We are just showing that the quantum interference process behind EIT has its equivalent in classical systems, where two or more normal modes interfere with each other to perform such phenomenologies. The patterns of interference observed in the mechanical scheme can be considerably useful to provide a general mapping of EIT-like systems into a variety of classical systems for practical device applications without the necessity of sophisticated technologies required for atomic systems.

APPENDIX

1. The dynamics of two coupled harmonic oscillators

In this Appendix we used the Hamiltonian formalism to show that, in addition to the steady-state solution of the EIT system, its dynamics is also equivalent to the dynamics of two coupled harmonic oscillators. Hence, we showed how to obtain ρ_{co}, drawn from the Newtonian formalism in Sec. II A, Eq. (15), using the Hamiltonian of the system.

If we recall from introductory physics that the total Hamiltonian for two coupled harmonic oscillators is obtained from the displacement x_j and linear momentum p_j of the jth oscillator as

$$H = \sum_{j=1}^{2} \left(\frac{p_j^2}{2m} + \frac{1}{2} m \omega_j^2 x_j^2 \right) - m \omega_{12}^2 x_1 x_2 - x_1 F_s(t), \quad \text{(A1)}$$

where we consider the masses to be equal to $m_{1,2} = m$, $\omega_j^2 = (k_j + k_{12})/m$ ($j = 1,2$), $\omega_{12}^2 = k_{12}/m$, and the force applied on oscillator 1, $F_s(t) = F e^{-i(\omega_s + \phi_s)t} + \text{c.c.}$ for $\phi_s = 0$, as illustrated in Fig. 1(b). By defining the classical variables $\alpha = (m\omega_1 x_1 + ip_1)/\sqrt{2\hbar m \omega_1}$ and $\beta = (m\omega_2 x_2 + ip_2)/\sqrt{2\hbar m \omega_2}$ and considering the simplified case where the natural frequencies of the oscillators are the same, $\omega_{1,2} = \omega$, meaning that $k_{1,2} = k$, the equation above for $\hbar = 1$ takes the form

$$H = \omega(\alpha^* \alpha + \beta^* \beta) - \frac{\omega_{12}^2}{2\omega}(\alpha^* \beta^* + \alpha\beta + \alpha^* \beta + \alpha\beta^*)$$
$$- \sqrt{\frac{F^2}{2m\omega}}(\alpha^* + \alpha)(e^{i\omega_s t} + e^{-i\omega_s t}). \quad \text{(A2)}$$

As in Eq. (13), the coupling rate between particles 1 and 2 is defined as $\Omega_{12} = \omega_{12}^2/2\omega$. Here we are able to find a direct expression for the pumping rate Ω_s as a function of the parameters of the classical system without the necessity of considering the constant C_1, like in Eq. (14). From Eq. (A2) we have $\Omega_s = \sqrt{F^2/2m\omega}$, which is analogous to the Rabi frequency of the probe field (Ω_p).

Now we make an approximation in order to discard fast oscillatory terms like $e^{\pm 2i\omega_s t}$ for $\omega \approx \omega_s$. This is similar to the RWA used in the quantum case. By performing the transformation $\alpha(t) = \tilde{\alpha}(t)e^{-i\omega t}$, likewise for β, we have

$$H = \omega(\alpha^* \alpha + \beta^* \beta) - \Omega_{12}(\alpha^* \beta + \alpha\beta^*)$$
$$- \Omega_s(\alpha e^{i\omega_s t} + \alpha^* e^{-i\omega_s t}). \quad \text{(A3)}$$

From the Poisson brackets $\dot{\rho} = \{\rho, H\} = -i\partial H/\partial \rho^*$ ($\rho = \alpha, \beta$) the time evolution of α and β are given by

$$\dot{\alpha} = -i(\omega\alpha - \Omega_{12}\beta - \Omega_s e^{-i\omega_s t} - i\gamma_1\alpha), \quad \text{(A4a)}$$
$$\dot{\beta} = -i(\omega\beta - \Omega_{12}\alpha - i\gamma_2\beta), \quad \text{(A4b)}$$

where we have added phenomenologically the dissipation terms γ_1 and γ_2 in analogy to the master equation formalism. By performing the transformation $\alpha(t) = \rho_\alpha(t)e^{-i\omega_s t}$ the same way for β, Eqs. (A4) are written as

$$\dot{\rho}_\alpha = -i\{(\Delta_s - i\gamma_1)\rho_\alpha - \Omega_{12}\rho_\beta - \Omega_s\}, \quad \text{(A5a)}$$
$$\dot{\rho}_\beta = -i\{(\Delta_s - i\gamma_2)\rho_\beta - \Omega_{12}\rho_\alpha\}, \quad \text{(A5b)}$$

with $\Delta_s = \omega - \omega_s$. Note that the equations above are completely equivalent to Eqs. (7) for ρ_{31} and ρ_{21}, respectively, if we consider the stationary solution $\dot{\rho}_{\alpha,\beta}(t) = 0$. It shows that the dynamics of both systems, EIT and coupled oscillators, are also equivalent with $\rho_{31} \equiv \rho_\alpha$ and $\rho_{21} \equiv \rho_\beta$. In the steady state Eqs. (A5) gives for ρ_α

$$\rho_\alpha(\omega_s) = \frac{\Omega_s(\Delta_s - i\gamma_2)}{(\Delta_s - i\gamma_1)(\Delta_s - i\gamma_2) - \Omega_{12}^2}, \quad \text{(A6)}$$

showing that $\rho_\alpha = \rho_{co}$ for $\Delta_{1,2} = \Delta_s$ in Eq. (14), as expected, once the Hamiltonian is equivalent to the Newtonian formalism.

2. The classical dark state

Here we explain the physics underlying the classical dark state for two coupled harmonic oscillators. For this we used the concepts of normal coordinates and normal modes to describe the collective motion of the system. This state is obtained when oscillator 1 is driven resonantly ($\omega_s = \omega_1$) by the harmonic force $F_s(t)$, causing the cancellation of the reduced mechanical susceptibility $\tilde{\chi}_M(\omega_s) = \rho_{co}(\omega_s)$ defined in Sec. II A. We consider the simple case where $m_{1,2} = m$ and $\omega_{1,2} = \omega$.

From the definition of the normal coordinates,

$$X_+ = (x_1 + x_2)/\sqrt{2}, \quad \text{(A7a)}$$
$$X_- = (x_1 - x_2)/\sqrt{2}, \quad \text{(A7b)}$$

and the normal momenta,

$$P_+ = (p_1 + p_2)/\sqrt{2}, \quad \text{(A8a)}$$
$$P_- = (p_1 - p_2)/\sqrt{2}, \quad \text{(A8b)}$$

the coupled Hamiltonian given in Eq. (A1) is now written as a combination of two uncoupled forced harmonic oscillators,

$$H_{nm} = \sum_{i=+,-} \left[\frac{P_i^2}{2m} + \frac{1}{2} m \omega_i^2 X_i^2 - \frac{\sqrt{2}}{2} F_s(t) X_i \right], \quad \text{(A9)}$$

where $\omega_+ = \sqrt{k/m}$ and $\omega_- = \sqrt{\omega_+^2 + 2\omega_{12}^2}$ are the resonance frequencies of the two normal modes of the system. Those are usually labeled as symmetric ($NM_{(+)}$) and asymmetric ($NM_{(-)}$) modes, owing the collective motion performed by each other. In $NM_{(+)}$ both masses move in phase with frequency ω_+ and the amplitudes are equal. In $NM_{(-)}$ both masses move oppositely, outward and then inward, with frequency ω_-, which is higher than ω_+ because the middle spring is now stretched or compressed adding its effect to the restoring force.

As we have seen, the equations of motion (11) described in Sec. II A are obtained by adding the damping force $-\eta_j \dot{x}_j$ to the resultant force of each oscillator, with $\eta_j = 2m\gamma_j$ ($j = 1,2$). From Eqs. (A1), (A7), and (A8) and the Hamilton equation,

$$\dot{p}_j = -\frac{\partial H}{\partial x_j} - 2m\gamma_j \dot{x}_j, \quad \text{(A10)}$$

the equations of motion for the normal coordinates are

$$\ddot{X}_+ + \Gamma \dot{X}_+ + \gamma \dot{X}_- + \omega_+^2 X_+ = \frac{F_s(t)}{m\sqrt{2}}, \quad \text{(A11a)}$$
$$\ddot{X}_- + \gamma \dot{X}_+ + \Gamma \dot{X}_- + \omega_-^2 X_- = \frac{F_s(t)}{m\sqrt{2}}, \quad \text{(A11b)}$$

with $\Gamma = (\gamma_1 + \gamma_2)$ and $\gamma = (\gamma_1 - \gamma_2)$. Note that the collective motions, provided by the normal modes, become uncoupled

for $\gamma_1 = \gamma_2$, once the coupling is performed through the asymmetric dissipation γ.

As before, we assume that the steady-state solution for the normal coordinates has the form $X_i = N_i e^{-i\omega_s t} +$ c.c., which conducts to the relationship

$$N_+ = \left[\frac{\omega_-^2 - \omega_s^2 + 2i\gamma_2\omega_s}{\omega_+^2 - \omega_s^2 + 2i\gamma_2\omega_s}\right]N_-. \qquad (A12)$$

Using the explicit values of ω_+ and ω_- defined previously, the classical dark state is obtained when $\omega_s = \omega$, with $\omega^2 = \omega_+^2 + \omega_{12}^2$. Then

$$N_+ = \left[\frac{\omega_{12}^2 - 2i\gamma_2\omega}{-\omega_{12}^2 - 2i\gamma_2\omega}\right]N_-. \qquad (A13)$$

Note that the system is pumped in a region of high interference between the normal modes, once $\omega_s = \omega$ is a frequency in the range between ω_+ and ω_-. To see how this state looks, we have to apply the classical analog for the EIT condition, which is $\Omega_{12} \gg \Omega_s$ and $\gamma_2 \ll \gamma_1$; see Sec. II A for more details. For $\gamma_2 \to 0$, Eq. (A13) provides $N_+ = -N_-$ and, consequently, $X_+ = -X_-$. From Eqs. (A7) it can be shown readily that $x_1 = \sqrt{2}/2(X_+ + X_-)$ and $x_2 = \sqrt{2}/2(X_+ - X_-)$. Note that the displacement of both oscillators can be described as a superposition of the two normal modes of the system. In this particular case, we have $x_1 = 0$ and $x_2 \neq 0$. Then the classical dark state is obtained when oscillator 1 stays stationary while oscillator 2 oscillates harmonically, meaning that it is featured by zero absorption power of oscillator 1. From Eq. (14) wee see that $\rho_{co}(\omega_s) \propto (N_+ + N_-)$, justifying why $\rho_{co}(\omega_s) = 0$ throughout the paper for zero detuning, like in Fig. 2.

The first EIT-like condition $\Omega_s \ll \Omega_{12}$ is demonstrated for $\gamma_2 \neq 0$. If $\gamma_2 \ll 1$, Eq. (A13) becomes

$$N_+ = -\left[1 - \frac{4i\gamma_2\omega}{\omega_{12}^2}\right]N_-. \qquad (A14)$$

The condition above is equivalent to $\gamma_2 \ll \gamma_1$, because all parameters of the system are scaled to γ_1. In this case the classical dark state remains observable when $k_{12} \gg k_1$, which implies that $\omega \approx \omega_{12} = \sqrt{k_{12}/m}$ and then $N_+ \approx -N_-$. If the frequency ω of the driven oscillator is taken from the expressions for the classical pumping $\Omega_s = \sqrt{F^2/2m\omega}$ and coupling $\Omega_{12} = \omega_{12}^2/2\omega$ rates, we have $\Omega_s = F\sqrt{\Omega_{12}/k_{12}}$. In the usual approximation of small oscillations the strength of the force, given by the amplitude F, is very small. Then, if $k_{12} \gg 1$, which is fulfilled for $k_{12} \gg k_1$, the condition $\Omega_s \ll \Omega_{12}$ must be prescribed for $\gamma_2 \neq 0$, in analogy to the EIT system, where $\Omega_p \ll \Omega_c$, since $\gamma_2 \ll \gamma_{31}$ for nonvanishing γ_2.

Thus, we show that the classical dark state is caused by a destructive interference between the normal modes $NM_{(\pm)}$ in the displacement of oscillator 1, and it is observed in analogous conditions with the dark state of the EIT system. The normal modes description performed here can be extended to the case of three coupled harmonic oscillators, as discussed in Sec. III, where the classical dark state is defined according to the configuration of the system.

[1] S. E. Harris, Phys. Today **50**, 36 (1997).
[2] J. P. Marangos, J. Mod. Opt. **45**, 471 (2009).
[3] M. Fleischhauer, A. Imamoglu, and J. P. Marangos, Rev. Mod. Phys. **77**, 633 (2005).
[4] L. V. Hau, S. E. Harris, Z. Dutton, and C. H. Behroozi, Nature (London) **397**, 594 (1999).
[5] M. M. Kash, V. A. Sautenkov, A. S. Zibrov, L. Hollberg, G. R. Welch, M. D. Lukin, Y. Rostovtsev, E. S. Fry, and M. O. Scully, Phys. Rev. Lett. **82**, 5229 (1999).
[6] D. Budker, D. F. Kimball, S. M. Rochester, and V. V. Yashchuk, Phys. Rev. Lett. **83**, 1767 (1999).
[7] J. Vanier, Appl. Phys. B **81**, 421 (2005).
[8] C. L. G. Alzar, M. A. G. Martinez, and P. Nussenzveig, Am. J. Phys. **70**, 37 (2002).
[9] P. R. Hemmer and M. G. Prentiss, J. Opt. Soc. Am. B **5**, 1613 (1988).
[10] A. G. Litvak and M. D. Tokman, Phys. Rev. Lett. **88**, 095003 (2002).
[11] G. S. Agarwal and S. Huang, Phys. Rev. A **81**, 041803(R) (2010).
[12] J. Harden, A. Joshi, and J. D. Serna, Eur. J. Phys. **32**, 541 (2011).
[13] Z. Bai, C. Hang, and G. Huang, Opt. Commun. **291**, 253 (2013).
[14] N. Papasimakis, V. A. Fedotov, N. I. Zheludev, and S. L. Prosvirnin, Phys. Rev. Lett. **101**, 253903 (2008).
[15] P. Tassin, L. Zhang, Th. Koschny, E. N. Economou, and C. M. Soukoulis, Phys. Rev. Lett. **102**, 053901 (2009).
[16] S.-Y. Chiam, R. Singh, C. Rockstuhl, F. Lederer, W. Zhang, and A. A. Bettiol, Phys. Rev. B **80**, 153103 (2009).

[17] N. Liu, L. Langguth, T. Weiss, J. Kästel, M. Fleischhauer, T. Pfau, and H. Giessen, Nat. Mat. **8**, 758 (2009).
[18] C. Kurter, P. Tassin, L. Zhang, Th. Koschny, A. P. Zhuravel, A. V. Ustinov, S. M. Anlage, and C. M. Soukoulis, Phys. Rev. Lett. **107**, 043901 (2011).
[19] Y. Sun, W. Tan, L. Liang, H.-T. Jiang, Z.-G. Wang, F.-Q. Liu, and H. Chen, Eur. Phys. Lett. **98**, 64007 (2012).
[20] T. J. Kippenberg and K. J. Vahala, Opt. Express **15**, 17172 (2007).
[21] J. M. Dobrindt, I. Wilson-Rae, and T. J. Kippenberg, Phys. Rev. Lett. **101**, 263602 (2008).
[22] S. Weis, R. Rivière, S. Deléglise, E. Gavartin, O. Arcizet, A. Schliesser, and T. J. Kippenberg, Science **330**, 1520 (2010).
[23] A. H. Safavi-Naeini, T. P. M. Alegre, J. Chan, M. Eichenfield, M. Winger, Q. Lin, J. T. Hill, D. E. Chang, and O. Painter, Nature (London) **472**, 69 (2011).
[24] X. Yang, M. Yu, D.-L. Kwong, and C. W. Wong, Phys. Rev. Lett. **102**, 173902 (2009).
[25] F. Liu, M. Ke, A. Zhang, W. Wen, J. Shi, Z. Liu, and P. Sheng, Phys. Rev. E **82**, 026601 (2010).
[26] X. Zhou, L. Zhang, W. Pang, H. Zhang, Q. Yang, and D. Zhang, New J. Phys. **15**, 103033 (2013).
[27] M. Mücke, E. Figueroa, J. Bochmann, C. Hahn, K. Murr, S. Ritter, C. J. Villas-Boas, and G. Rempe, Nature (London) **465**, 755 (2010).
[28] D. B. Sullivan and J. E. Zimmerman, Am. J. Phys. **39**, 1504 (1971).

[29] H. J. Maris and Q. Xiong, Am. J. Phys. **56**, 1114 (1988).

[30] B. W. Shore, M. V. Gromovyy, L. P. Yatsenko, and V. I. Romanenko, Am. J. Phys. **77**, 1183 (2009).

[31] W. Frank and P. von Brentano, Am. J. Phys. **62**, 706 (1994).

[32] L. Novotny, Am. J. Phys. **78**, 1199 (2010).

[33] R. Marx and S. J. Glaser, J. Magn. Reson. **164**, 338 (2003).

[34] V. Leroy, J.-C. Bacri, T. Hocquet, and M. Devaud, Eur. J. Phys. **27**, 1363 (2006).

[35] J. L. McKibben, Am. J. Phys. **45**, 1022 (1977).

[36] A. Eisfeld and J. S. Briggs, Phys. Rev. E **85**, 046118 (2012).

[37] J. S. Briggs and A. Eisfeld, Phys. Rev. A **85**, 052111 (2012).

[38] Although the complexity of realistic atoms, which are composed of a multilevel energy structure, optical pumping techniques are used to adequately produce two-, three-, or four-level atoms. This makes the modeling of simple energy structures configurations, such as the systems presented here, reasonable.

[39] R. W. Christy, Am. J. Phys. **40**, 1403 (1972).

[40] A. Lipson, S. G. Lipson, and H. Lipson, *Optical Physics*, 4th ed. (Cambridge University Press, Cambridge, UK, 2011).

[41] M. A. de Ponte, C. J. Villas-Boas, R. M. Serra, and M. H. Y. Moussa, Europhys. Lett. **72**, 383 (2005).

[42] M. O. Scully and M. S. Zubairy, *Quantum Optics* (Cambridge University Press, Cambridge, UK, 1997).

[43] L. E. Estes, T. H. Keil, and L. M. Narducci, Phys. Rev. **175**, 286 (1968).

[44] P. R. Rice and R. J. Brecha, Opt. Commun. **126**, 230 (1996).

[45] H. J. Carmichael, L. Tian, W. Ren, and P. Alsing, in *Cavity Quantum Electrodynamics*, edited by P. R. Berman (Academic Press, Boston, 1994), pp. 381–423.

[46] S. M. Tan, J. Opt. B: Quantum Semiclass. Opt. **1**, 424 (1999).

[47] C. Sames, H. Chibani, C. Hamsen, P. A. Altin, T. Wilk, and G. Rempe, Phys. Rev. Lett. **112**, 043601 (2014).

[48] A. Joshi and M. Xiao, Phys. Lett. A **317**, 370 (2003).

[49] C. Goren, A. D. Wilson-Gordon, M. Rosenbluh, and H. Friedmann, Phys. Rev. A **69**, 063802 (2004).

[50] S. Rebić, D. Vitali, C. Ottaviani, P. Tombesi, M. Artoni, F. Cataliotti, and R. Corbalàn, Phys. Rev. A **70**, 032317 (2004).

[51] D. Petrosyan and Y. P. Malakyan, Phys. Rev A **70**, 023822 (2004).

[52] S. Li, X. Yang, X. Cao, C. Zhang, C. Xie, and H. Wang, Phys. Rev. Lett. **101**, 073602 (2008).

[53] M. D. Lukin, M. Fleischhauer, M. O. Scully, and V. L. Velichansky, Opt. Lett. **23**, 295 (1998).

[54] G. Hernandez, J. Zhang, and Y. Zhu, Phys. Rev. A **76**, 053814 (2007).

[55] H. Wu, J. Gea-Banacloche, and M. Xiao, Phys. Rev. Lett. **100**, 173602 (2008).

[56] J. A. Souza, E. Figueroa, H. Chibani, C. J. Villas-Boas, and G. Rempe, Phys. Rev. Lett. **111**, 113602 (2013).